



National Aeronautics and
Space Administration

NASA CR-151978

(NASA-CR-151978) JOULE-THOMSON EXPANDER AND
HEAT EXCHANGER Final Technical Report
(AiResearch Mfg. Co., Torrance, Calif.)
67 p HC A04/EF A01

N77-22424

CSCI 20D

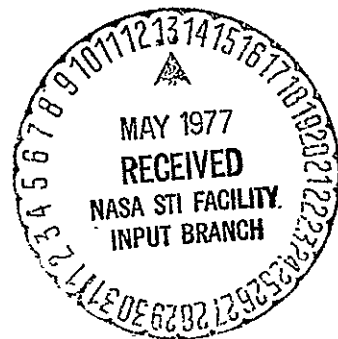
Unclas
27961

G3/34

FINAL TECHNICAL REPORT ON JOULE-THOMSON EXPANDER AND HEAT EXCHANGER

AiResearch Manufacturing Company
of California

November 17, 1976



Prepared for

National Aeronautics and Space Administration
Ames Research Center
Moffett Field, California 94035

FINAL TECHNICAL REPORT ON JOULE-THOMSON EXPANDER AND HEAT EXCHANGER

**AiResearch Manufacturing Company
of California**

November 17, 1976

Prepared for

**National Aeronautics and Space Administration
Ames Research Center
Moffett Field, California 94035**

FOREWORD

The Joule-Thomson Expander and Heat Exchanger Program was performed under NASA Contract NAS2-8984, by the AiResearch Manufacturing Company of California, a division of The Garrett Corporation. This work was sponsored by the Ames Research Center, Moffett Field, California, and administered under the direction of Mr. John Vorreiter, M/S 244-14.

This report was prepared by Mr. R. H. Norman, who was responsible for the analytical effort. Mr. J. R. Wenker was responsible for the development and fabrication of the assemblies, under the Program direction of Mr. O. A. Buchmann.

CONTENTS

<u>Section</u>		<u>Page</u>
1	INTRODUCTION AND SUMMARY	1-1
	Introduction	1-1
	Program Requirements	1-1
	Summary	1-1
2	DESIGN AND FABRICATION	2-1
	JTX No. 1	2-1
	JTX No. 2	2-3
	JTX No. 3	2-7
	Flow Calibration Tests	2-7
3	PERFORMANCE ANALYSIS	3-1
	J-T Thermodynamics	3-1
	Computer Program Development	3-1
	JTX No. 1 Performance Prediction	3-10
	JTX No. 1 Test Data Analysis	3-13
	JTX No. 2 Performance Prediction	3-17
	JTX No. 3 Performance Prediction	3-18
	REFERENCES	R-1
 <u>Appendix</u>		
A	COMPUTER PROGRAM	A-1
B	THERMOPHYSICAL PROPERTIES	B-1

SECTION 1

INTRODUCTION AND SUMMARY

SECTION 1

INTRODUCTION AND SUMMARY

INTRODUCTION

The Joule-Thomson Expander and Heat Exchanger Program provides for the design, fabrication, and delivery of three assemblies, each consisting of the following components; the combination thereof referred to as a JTX:

- Inlet filter
- Counterflow heat exchanger
- Joule-Thomson expansion device
- Low-pressure jacket

The program objective was to develop a JTX, which, when coupled to an open-cycle supercritical helium refrigerating system (i.e., a storage vessel), would supply superfluid helium (He II) at 2 K or less, for cooling infrared detectors.

PROGRAM REQUIREMENTS

A four-task program was originally planned, including two additional design iterations based on testing by the Government. The first task was design of a JTX assembly to provide 30 milliwatts of cooling at 2 K. The second task was a performance analysis (prediction) of the JTX over a range of helium inlet temperatures and pressures. The third task was fabrication and delivery of an assembly to the Government for testing. The second JTX design was to await the test results of the first; similarly, the third design was to await the test results of the second. The fourth task was submittal of a final technical report after the two design iterations were completed.

These requirements were somewhat modified since the inception of the program. All three tasks were carried out for JTX No. 1. JTX No. 2 has been fabricated and delivered, but not tested. The design of JTX No. 3 was redirected to satisfy the requirements of an astronomical detector cooling system, as specified by an amendment to this contract.

SUMMARY

All three cryostats were designed; the first, JTX No. 1, was tested and returned for modifications. This modified assembly, designated JTX No. 1A, was then delivered to the Government. The second cryostat was fabricated, flow-tested with nitrogen, and delivered; the third has been designed.

The design of all units was based on existing technology developed for nitrogen J-T cryostats, with a minor modification to the expansion device. The primary design tool for He II cryostats is a JTX Performance Prediction Program. Test data has essentially verified the computer model although the capillary tube characterization still is difficult for certain input conditions. The computer program was modified several times as flow calibration data became available, but the basic elements remain the same for JTX No. 3 as they were for JTX No. 1.

The test data for JTX No. 1 successfully demonstrated the formation of superfluid He II at 1.85 K. The test instrumentation, however, did not enable a direct comparison of heat exchanger performance to computer predictions except for flow rate and cooling capacity. The test flow rate was about 50 percent higher than predicted. There are several possible explanations for this: one is the tolerance in capillary tube diameter (a 20 percent increase above nominal could give 50 percent more flow); another is the possible formation of superfluid in the capillary which is not modeled in the computer program.

JTX No. 2 was to be identical to JTX No. 1 except for replacing the small capillary tube with another of the same diameter having twice the length. At this point it was established that the original 0.0508 mm (0.002 in.) I.D. capillary tubing was no longer available (except by special mill run). A substitute of 0.102 mm (0.004 in.) I.D. tubing was approved. The unit was fabricated, nitrogen flowtested, and delivered. The room-temperature nitrogen flow test showed that JTX No. 2 had about half the flow capacity of JTX No. 1, which was the desired effect.

The modified JTX No. 1A was to have the same capillary tube replacement as JTX No. 2. In the absence of 0.0508 mm I.D. tubing, 0.0838 mm (0.0033 in.) tubing was used. A nitrogen flow test showed JTX No. 1A to have about half the flow capacity of JTX No. 2.

JTX No. 3 was designed for use in the optical cavity dewar of an Astronomical. Detector Cooling System, for which a preliminary design was conducted under Contract Amendment No. 1. This system design was completed and documented in a separate report (Reference 1). JTX No. 3 was designed to produce 100 milliwatts of cooling at 2 K with inlet conditions of 13.6 atm (200 psia) and 17 K.

SECTION 2
DESIGN AND FABRICATION

SECTION 2

DESIGN AND FABRICATION

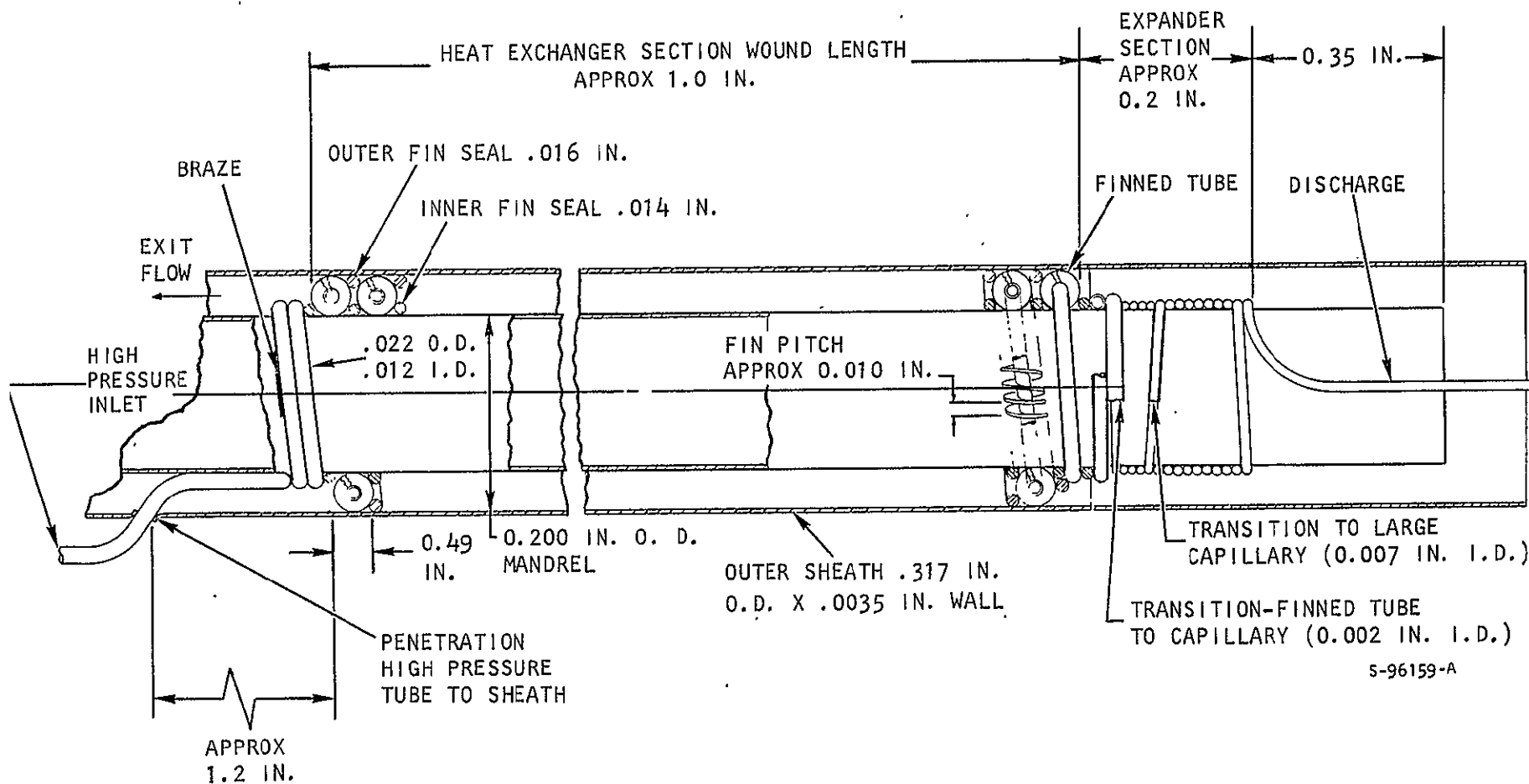
JTX NO. 1

The JTX assembly consists of the following components:

- Mandrel and closure
- Sheath (low-pressure jacket)
- High-pressure tubing, partly finned
- Expander (2 capillary tubes in series)
- Fin seals
- Inlet filter
- GFE flanges

The JTX design is derived from existing technology developed for nitrogen Joule-Thomson cryostats. All of the components listed above are essentially the same as a nitrogen J-T cryostat with the exception of the J-T expander. With nitrogen cryostats operating between 150 atm and 1 atm, a single expansion capillary is used. To expand supercritical helium (5 to 20 atm) to the low pressures required to produce superfluid helium II (2 to 20 torr, 0.0026 to 0.026 atm) in a single capillary tube would result in extremely high exit velocities and relatively high exit-expansion losses. It is believed that a two-step expansion process, where a larger capillary tube is attached to the end of a smaller one, promotes a more controlled expansion into the vacuum of the cooling cavity.

The JTX assembly, without flanges and filter, is presented in Figure 2-1, showing the approximate dimensions for JTX No. 1. The mandrel is a seamless tube of L605 (Haynes Alloy 25), a high cobalt alloy with desirably low thermal conductivity and heat capacity. The mandrel is sealed at the cold end to prevent helium flow from bypassing the finned tube heat exchanger. The sheath is also fabricated of L605 alloy thin-wall tubing. The diameter is selected for proper mandrel-to-sheath gap for the selected fin. The copper fin is formed from 0.203 mm (0.008 in.) diameter wire to dimensions of approximately 0.104 mm (0.0041 in.) by 0.318 mm (0.0125 in.) and annealed. A post heat-treat cleaning is performed prior to winding the fin. The high-pressure tubing of 300-series stainless steel of 0.559 mm (0.022 in.) O.D. by 0.305 mm (0.012 in.) I.D. is cut to extra length and cleaned to remove contaminants which could react in the brazing cycle. Following internal cleaning the tubing is crimped shut and externally cleaned and plated. Copper and silver are plated onto the high-pressure tube to provide braze material for the silver-copper eutectic which bonds the fin to the tube. The copper fin is then edge-wound over the high pressure tube, with a slight excess temporarily tack-soldered at each end to hold it in place. The fin spacing is controlled to about 39



5-96159-A

Figure 2-1. Design Details of JTX No. 1 (Without Flanges)

fins/cm (100 fins/in.). The wound finned tube is then brazed in an inert atmosphere to secure the fin to the tube with a thermally conductive joint. A careful visual inspection of the braze fillets is made to assure that a proper fin-to-tube bond exists. A short length of unfinned tube is wound around the mandrel and tack-brazed at each end. The high-pressure tube is then cut to reopen it, and the first section of capillary tube is inserted a short distance in and sealed with a braze joint. This capillary tube is of 300-series stainless steel with nominal dimensions of 0.153 mm (0.006 in.) O.D. by 0.0508 mm (0.002 in.) I.D.* by 7.4 cm (2.9 in.) long. The second capillary tube is slipped over the first, sealed with a braze, and the two are wrapped onto the mandrel and secured with soft solder. The nominal dimensions of this second capillary are 0.330 mm (0.013 in.) O.D. by 0.178 mm (0.007 in.) I.D. by 22 cm (8.5 in.) long. The finned tube and expansion capillaries are then wrapped around the mandrel. The inner fin seal, 0.356 mm (0.014 in.) diameter nylon, is installed and adjusted to provide the proper fin pitch and outside diameter. The nominal O.D. of the fin is 1.25 mm (0.049 in.), therefore approximately 20 coils provides the required 40 cm (15.8 in.) length of finned tube, occupying about 2.5 cm (1.0 in.) of mandrel length. The outer fin seal, 0.406 mm (0.016 in.) diameter nylon, is then installed and secured. The wrapped heat exchanger section is then carefully sized using tooling to ensure that the wrap is uniform and will properly contact the sheath. The fin seals are used to direct the low pressure helium away from the sheath and mandrel and into better contact with the finned tube.

The photograph in Figure 2-2 shows the final assembly of heat exchanger and expansion tube wound around the mandrel. The sheath with GFE flanges and inlet heater are shown beside the heat exchanger/expander subassembly in Figure 2-3. The large upper flange contains the instrumentation feedthrough provisions and the lower smaller flange mates to the sensor mounting plate. The helically coiled tube between the flanges contains the JTX inlet electrical heater. The photograph of Figure 2-4 shows the completed JTX assembly, prior to installation of sensors and instrumentation. The soldered sheath penetration of the inlet tube can be seen just below the helical heater. Above the large flange is the inlet filter assembly fitted to a 0.318 cm (1/8 in.) O.D. supply line. This filter is of the stainless steel sintered-mesh type with a nominal 2 micron rating.

The modified JTX assembly, JTX No. 1A, was identical in design to JTX No. 1 with the exception of the expansion capillary tubes. A small capillary tube which measured (single microsection) 0.185 mm (0.0073 in.) O.D. by 0.0838 mm (0.0033 in.) I.D. by 60 cm (23.6 in.) long, was installed. The larger capillary tube was replaced by a 30 cm (12 in.) length of 0.457 mm (0.018 in.) O.D. by 0.254 mm (0.010 in.) I.D. tubing (not measured).

JTX NO. 2

The second assembly, JTX No. 2, was identical to JTX No. 1, except for the expander. In this unit a small capillary of nominal dimensions 0.203 mm

*An approximate measurement of this tubing from a 400X photograph revealed 0.007 in. O.D. by 0.0024 to 0.0026 in. I.D.

REPRODUCIBILITY OF THE
ORIGINAL PAGE IS POOR

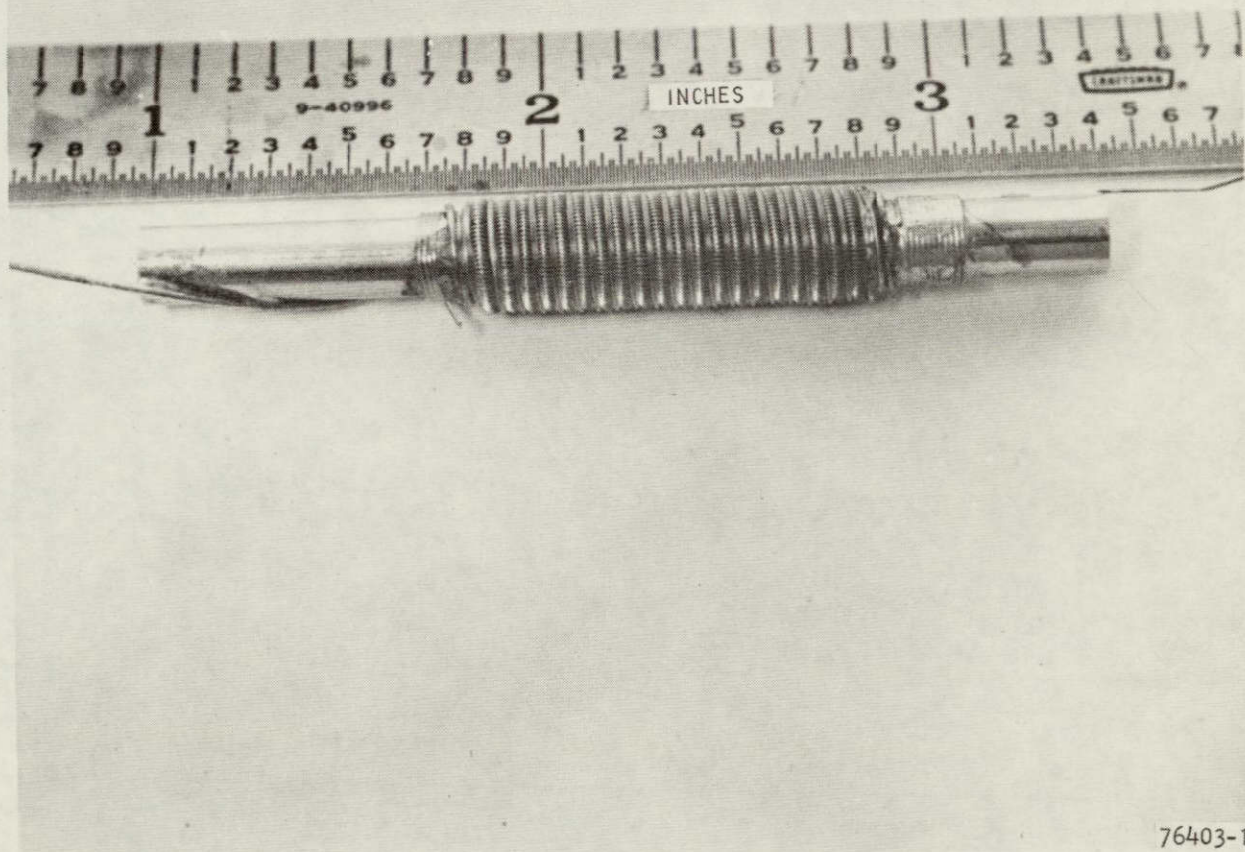
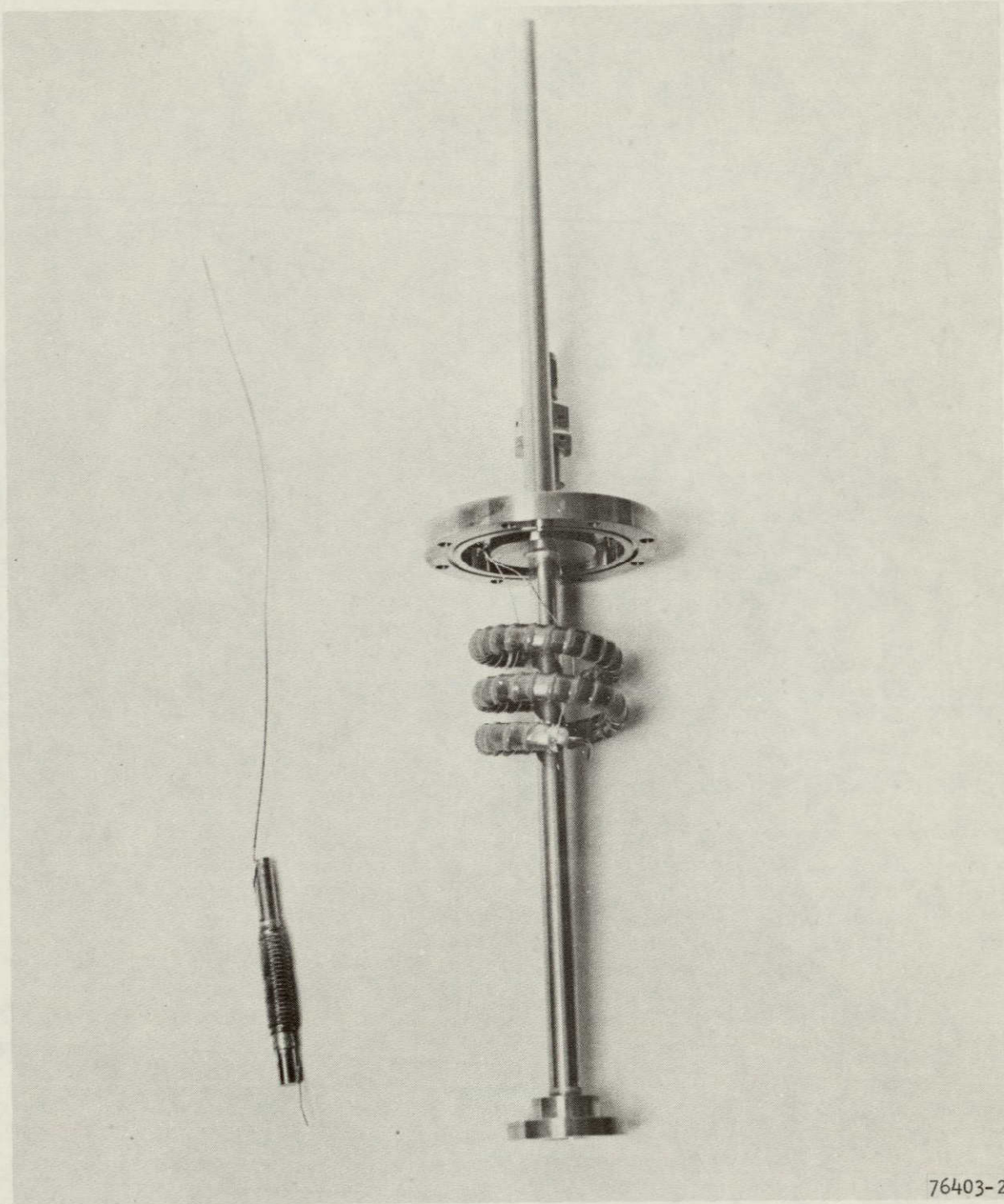


Figure 2-2. J-T Expander and Heat Exchanger Wound on Mandrel



AIRESEARCH MANUFACTURING COMPANY
OF CALIFORNIA



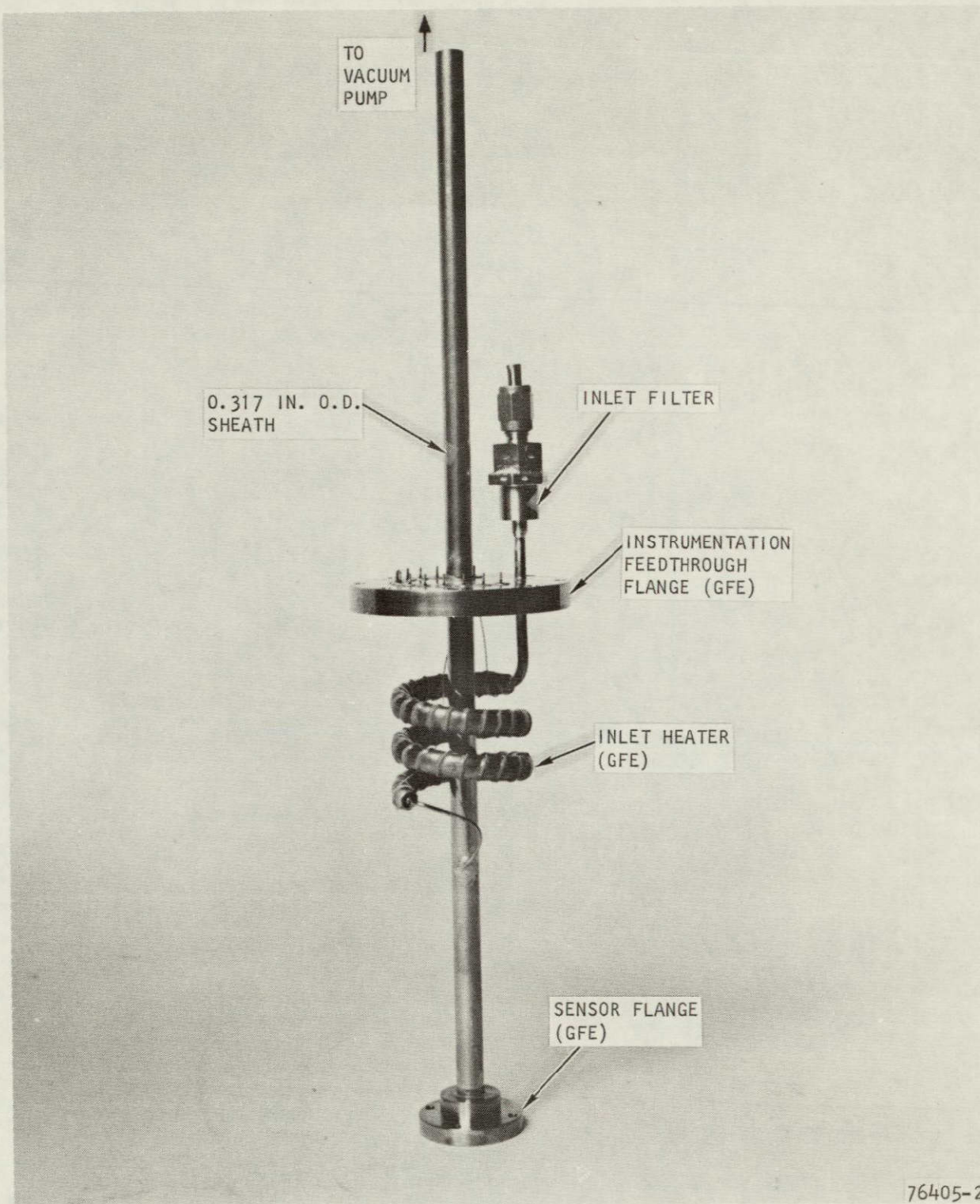
76403-2

Figure 2-3. J-T Expander and Heat Exchanger with Sheath, Flanges and Inlet Heater



AIRESEARCH MANUFACTURING COMPANY
OF CALIFORNIA

76-13285
Page 2-5



76405-2

F-24545

Figure 2-4. Completed JTX Assembly



AIRESEARCH MANUFACTURING COMPANY
OF CALIFORNIA

76-13285
Page 2-6

REPRODUCIBILITY OF THE
ORIGINAL PAGE IS POOR

(0.008 in.) O.D. by 0.102 mm (0.004 in.) I.D. by 86 cm (34 in.) long was installed. The large capillary tube was the same size as that used on JTX No. 1A. The actual measurements from a microsection of the small capillary tube were 0.0081-0.0082 in. O.D. by 0.0044-0.0046 in. I.D.

The sheath, flanges, and inlet filter were assembled around the wrapped mandrel, as with JTX No. 1, but the helically coiled heater was omitted. An extended length of inlet tubing was provided between the upper flange and the point of sheath penetration.

JTX NO. 3

The third JTX assembly was designed to provide cooling for infrared detectors in an optical cavity dewar of the Astronomical Detector Cooling System (Reference 1). The design is essentially the same as that for the preceding two cryostats with the following exceptions. The finned tubing of the heat exchanger is longer: the total length is 61 cm (24 in.), occupying about 4.1 cm (1.6 in.) of mandrel length. The expander capillary tubes are the same nominal sizes that were used on JTX No. 2, except that the length of the smaller tube is 46 cm (18 in.). The flanges, fittings, inlet filter, and sheath assembly are all different than in previous JTX's in order to be installed in the relatively small envelope of the optical cavity dewar. These details are shown in a layout drawing presented in Reference 1.

A summary of expander capillary tube sizes for all four assemblies is presented in Table 2-1.

FLOW CALIBRATION TESTS

After final assembly and cleaning of each JTX assembly, a flow test with ambient (room) temperature nitrogen and/or helium is performed. High-pressure gas is regulated into the JTX and vented through the expander, exhausting to atmospheric pressure. The flow rate is measured as a function of inlet pressure. At the moderate pressures used, the nitrogen cools very little upon J-T expansion. The helium, of course, warms insignificantly upon J-T expansion at room temperature.

These preliminary tests are performed to verify that the expander capillary is not plugged. In the production of nitrogen J-T cryostats for other applications this test is routinely performed to "calibrate" the capillary tube; that is, the required flow range is obtained by clipping off the capillary tube and re-testing. In the JTX application this calibration cannot be performed because of the lack of a cryogenic supply of supercritical helium and a special test setup. If liquid nitrogen were used, it would not verify He II performance without actually prior-testing with supercritical helium, anyway.

The JTX No. 1 assembly was flow-tested with helium and nitrogen. The other two assemblies, JTX No. 2 and JTX No. 1A were tested with nitrogen only. The four sets of data points are plotted in Figure 2-5, with the test data correlations obtained by linear regression analysis (a power curve fit was chosen, since the data plotted on a log-log scale indicated a straight line).

TABLE 2-1
SUMMARY OF EXPANDER CAPILLARY TUBE SIZES

Dimension	JTX Assembly			
	No. 1	No. 1A	No. 2	No. 3*
<u>Small Capillary Tube</u>				
Nominal I.D., mm	0.0508	?	0.102	0.102
in.	0.002		0.004	0.004
Nominal O.D., mm	0.153	?	0.203	0.203
in.	0.006		0.008	0.008
Measured I.D., mm	0.0635	0.0838	0.114	--
in.	0.0025**	0.0033	0.0045	--
Measured O.D., mm	0.178	0.185	0.208	--
in.	0.0070**	0.0073	0.0082	--
Length, cm	7.4	60	86	46
in.	2.9	23.6	34	18
<u>Large Capillary Tube</u>				
Nominal I.D., mm	0.178	0.254	0.254	0.254
in.	0.007	0.010	0.010	0.010
Nominal O.D., mm	0.330	0.457	0.457	0.457
in.	0.013	0.018	0.018	0.018
Length, cm	22	30	30	30
in.	8.5	12	12	12

*These sizes are design values used in performance prediction analysis

**Approximate measurement from photo of contaminated section

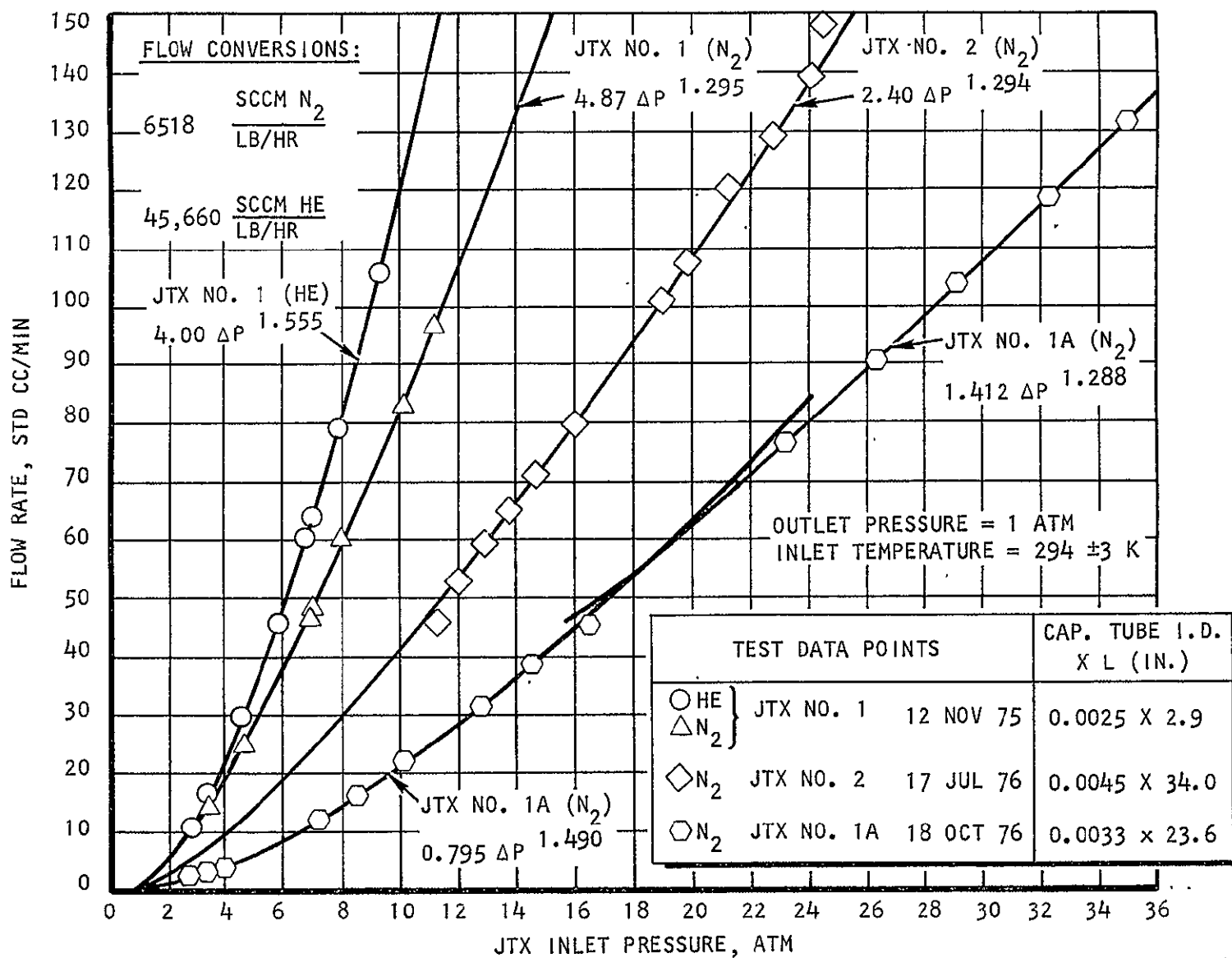


Figure 2-5. Correlation of Flow Calibration Test Data

In addition to the expander flow tests, a special nitrogen test was performed with JTX No. 2 to measure the pressure drop through the low-pressure side finned heat exchanger as a function of flow rate. This was accomplished by blocking the sheath on the expander end and attaching an inclined manometer to measure the pressure differential between the expander outlet and the atmosphere (the flow being exhausted out the sheath/mandrel annulus at the JTX inlet end). The purpose of this special test was to correlate the Zeta-factor in the analytical model to actual pressure-drop data. Again, the validity is limited by the measurements being taken with nitrogen at room temperature and atmospheric pressure, rather than helium at 4 to 20 K and subatmospheric pressure. An important result of this test was, nevertheless, the modification of the computer model to account for "laminar" flow around the fins, for very low Reynolds numbers. This will be discussed in the next section. Figure 2-6 shows the good correlation between the pressure-drop data and the laminar-flow-modified computer model, for a Zeta-factor of 0.748. This Zeta was obtained by reducing the pressure-drop data to Zeta-factors, and computing the arithmetic mean value (the standard deviation was ± 0.010).

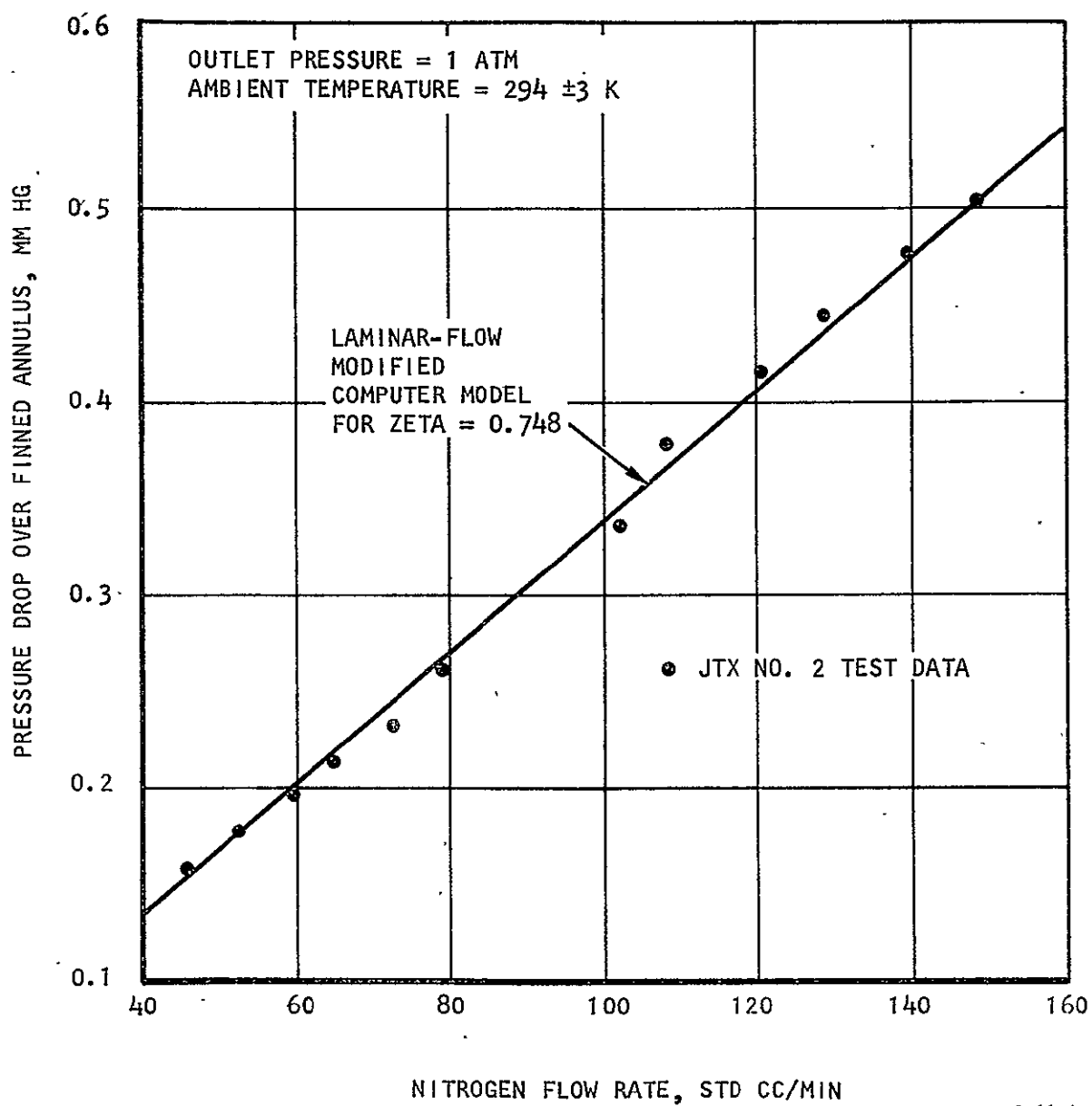


Figure 2-6. Correlation of Finned Annulus Pressure-Drop Test Data

SECTION 3
PERFORMANCE ANALYSIS

SECTION 3

PERFORMANCE ANALYSIS

J-T THERMODYNAMICS

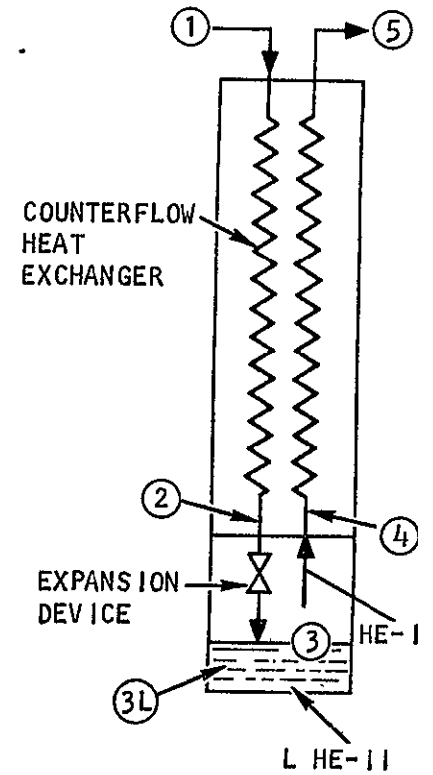
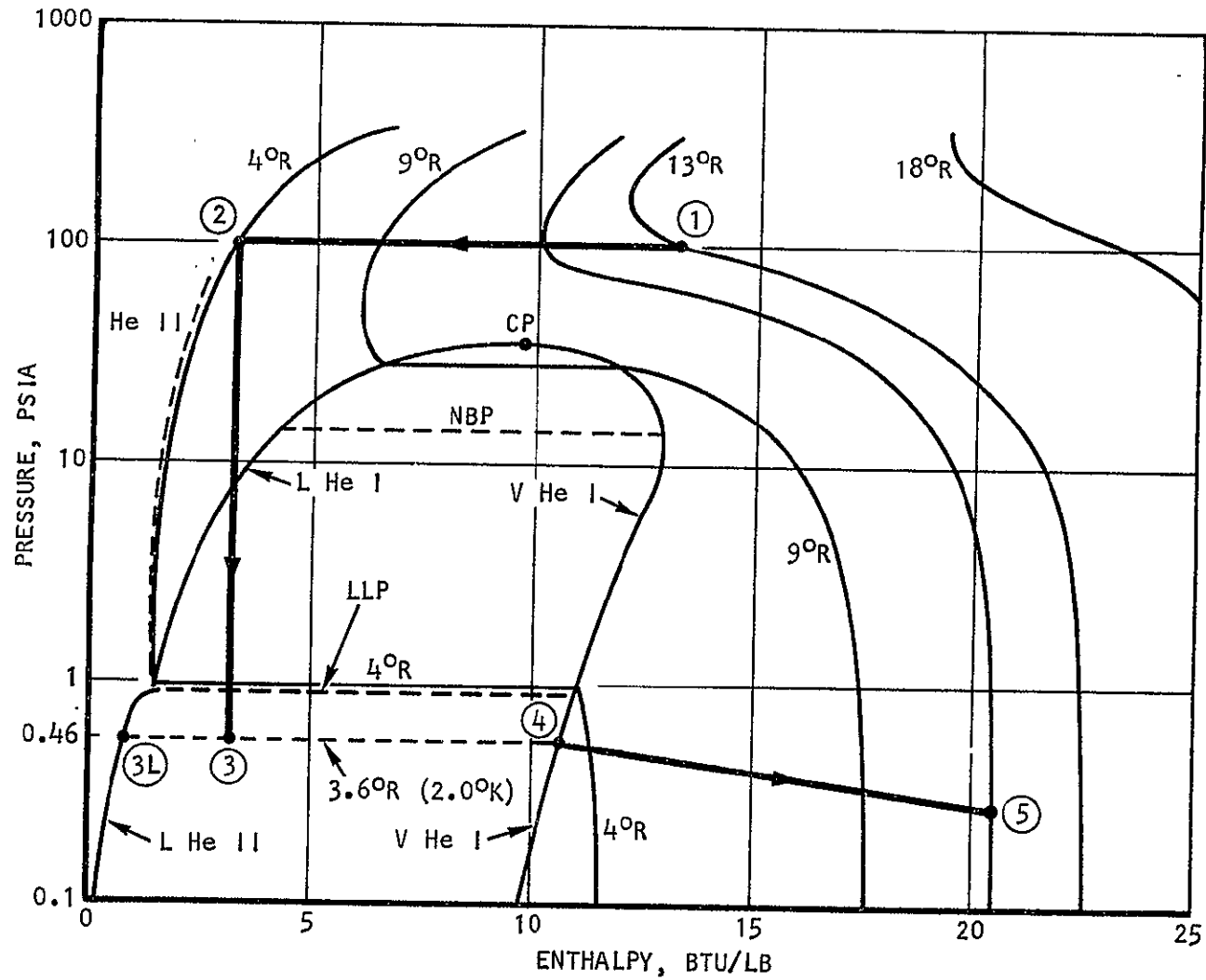
The Joule-Thomson (J-T) process can best be understood by examining a pressure-enthalpy diagram of the working fluid. Figure 3-1 presents a schematic of the J-T expander and heat exchanger, together with a gross representation of the pressure-enthalpy diagram for helium 4 in the low-temperature region. The diagram shows the state points corresponding to the key physical locations in the JTX as depicted in the schematic.

Briefly, the process consists of two heat exchange steps in which high-pressure gas is cooled (1 to 2) with low-pressure vapor (4 to 5) boiling out of the two-phase mixture (3); separated by an isenthalpic (adiabatic irreversible) expansion to a low pressure where coexisting liquid (He II, in this case) and vapor (He I) appear. The refrigeration load (IR sensor) and heat leak cause the vapor to boil off, returning to the heat exchanger, leaving behind the liquid phase to maintain a stable temperature level. The thermodynamics of this process imply that the formation of superfluid helium (He II) is possible if suitable expander inlet temperatures and chamber back pressures (vacuum level) are obtained.

COMPUTER PROGRAM DEVELOPMENT

A computer program, written in FORTRAN V language for the Univac 1108 computer (University Computing Company software), is used to predict the performance of a JTX of a given design (all geometrical parameters must be specified). The only operational parameters required are the heat exchanger high-pressure-side inlet pressure and temperature, and the refrigeration load temperature (which determines the helium pressure at the inlet to the low-pressure side of the counterflow heat exchanger). Helium thermophysical properties maps were assembled to cover the expected operating pressure and temperature ranges. The overall logic and operation of the computer program are discussed in this section, while a detailed summary of the key subroutines is presented in Appendix A. The development of a pressure-enthalpy diagram extending into the helium II region, and a tabulation all properties required by the program are presented in Appendix

A block diagram of the JTX computer program showing the subroutine structure is presented in Figure 3-2. There are four basic groups of routines under the main program (MAIN): (1) a data element containing the helium thermophysical properties (HELIUM/DATA)--specific enthalpy, specific volume, dynamic viscosity and thermal conductivity, each as a function of pressure and temperature, (2) a group of service routines for reading and looking up the helium properties (HEREAD, THERMO, etc.), (3) the main operational routines which perform the J-T cycle analysis (JTX) and characterize the pressure-drop and heat transfer performance (DPIHX, EXPDR, HEATX, etc), and (4) the purely mathematical iteration routine NEWTON, and its own service subroutines (LNMOD, MATMUL, etc), which performs the iteration on the two key system variables from which all other unknowns are directly calculated. The subroutine FENCE contains the limits imposed on the two independent variables converged upon by NEWTON.



S-11021

Figure 3-1. Joule-Thomson Expander and Heat Exchanger Operation

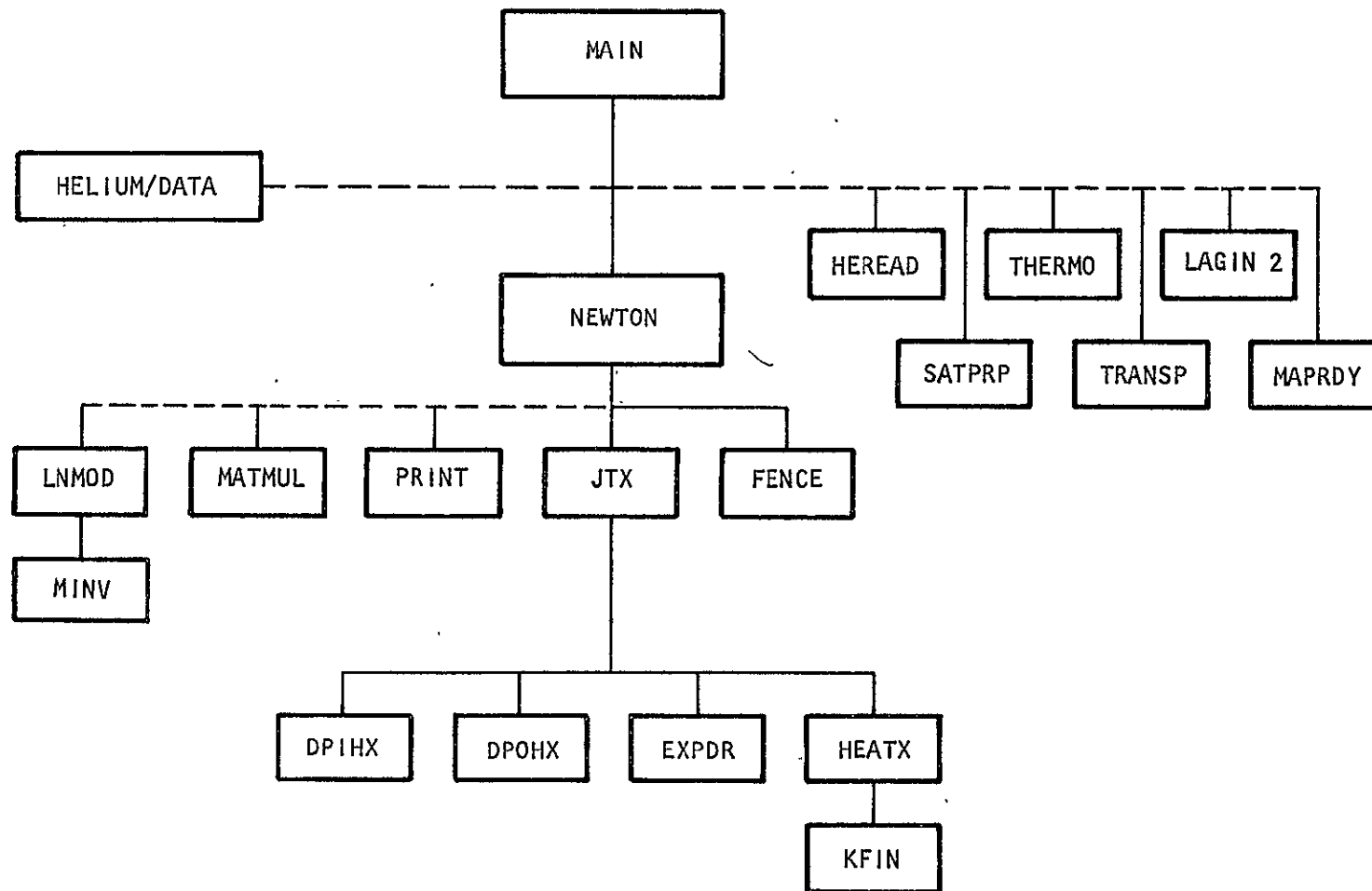


Figure 3-2. JTX Computer Program Subroutine Structure

S-11013

The two key variables (unknown) are expander inlet temperature and flow rate. The MAIN program provides a guess of each one and then calls NEWTON. This proprietary AiResearch program makes use of the so-called Newton-Jacobian matrix method of solving an array of unknowns by imposing stepwise incremental changes and examining the derivative of each function of that variable to obtain the next guess in the path toward convergence. NEWTON calls the subroutine JTX every time it obtains a new guess.

Subroutine JTX is the cycle analysis program which calculates the system pressure drops and heat exchanger performance, based on the guessed value of expander inlet temperature and flow rate. It starts from the high-pressure-side inlet conditions and calls DPIHX to compute pressure drop inside the coiled tube. This pressure drop subtracted from the JTX inlet pressure gives the inlet pressure to the expander. With the expander inlet conditions (P, T) known, EXPDR is called to calculate the pressure drop in the two capillary tubes. This is the most difficult calculation in the program because of the widely varying fluid properties from inlet to outlet. The procedure is to divide each tube into 20 increments of length and calculate the isenthalpic pressure drop in each segment by the conventional incompressible flow equation, assuming fluid properties are constant over the length increment. The friction factor correlation used in both DPIHX and EXPDR is taken from Reference 2, for turbulent flow in coiled tubing.

The pressure drop on the low-pressure side of the heat exchanger is computed by DPOHX, from the inlet conditions given by the cooling cavity. Saturated vapor at the refrigeration temperature enters the annulus and flows over the finned tubing. The friction factor correlation for flow around finned circular tubes is based on Reference 3, with the addition of a laminar-type flow dependence at very low Reynolds numbers. This subroutine makes use of the Zeta-factor in the calculation of flow area. This factor is determined from experimental data (see Figure 2-6), and attempts to account for the flow restriction caused by the presence of the fin seals, as well as the effect of continual expansion and contraction as the helium flows around the tube coils, fin seals, and between the fins.

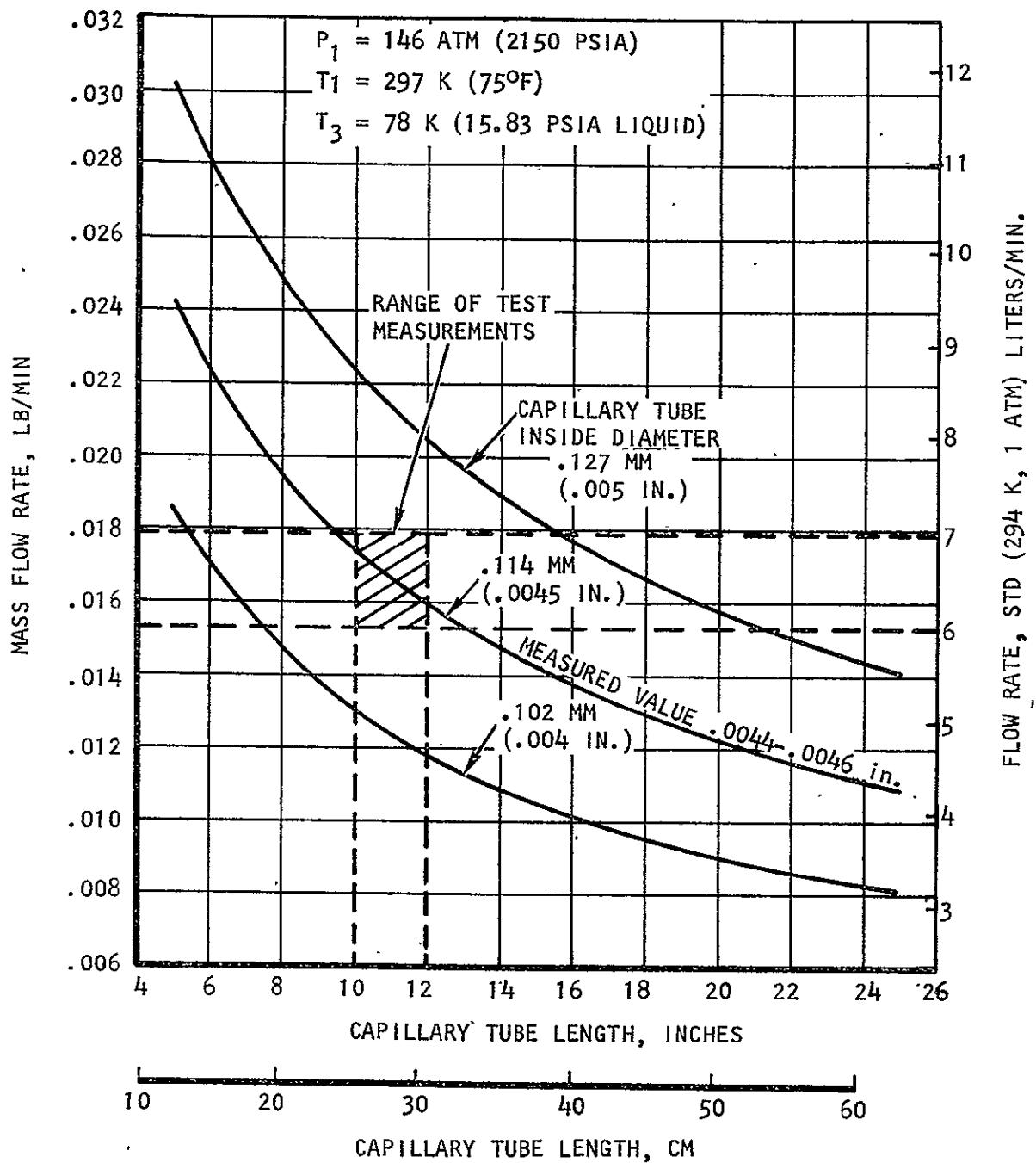
The heat exchanger performance is calculated by subroutine HEATX, given all the inlet and outlet conditions. At this point, the outlet temperature on the low-pressure side is obtained by heat balance over the heat exchanger. The output of HEATX is the overall thermal conductance, based on a coiled-tube heat transfer coefficient (inside tube) correlation from Reference 4, and a correlation for the outside finned tube coefficient from Reference 3. The overall conductance (UA) is then used to calculate the heat exchanger effectiveness, which in turn gives the low-pressure-side outlet temperature. This temperature, T_5 in Figure 3-1, is one of the convergence parameters. When the T_5 obtained from HEATX agrees with the T_5 obtained from the heat balance, then one of the convergence closures is satisfied. The other convergence closure is the expander pressure drop (ΔP_x), which is made to agree with the difference between the state point pressures P_2 and P_3 in Figure 3-1. In the development of the computer program, this latter convergence closure became the focus of much attention. In many early cases this closure failed to converge, while the T_5 convergence was excellent, and the cycle state points all seemed reasonable. Detailed study of the subroutine EXPDR (a stand-alone version was developed)

revealed that the expander pressure drop was extremely sensitive to flow rate, and the closer the flow rate was to the converged value, the more sensitive it became. Convergence was finally obtained for most cases by comparing the logarithm of the pressure differences, instead of the pressure differences themselves. The resulting flow rates were usually within a few percent of the unconverged value. This problem is believed to be caused by the large change in fluid properties (density and viscosity) over the range of pressures encountered in the expander; from supercritical, high-density fluid, passing very near the critical point, then into the two phase region where liquid and vapor coexist. At first, a conservative approach was taken by assuming that the viscosity of the two-phase mixture was the viscosity of the vapor only. This apparently created large discontinuities between two successive length increments, making convergence more difficult. To obtain a higher percentage of converged results, a mixed-mean or "homogenized", viscosity value was used. The mixed value is simply the mass-weighted average of the liquid and vapor values.

As will be shown later, this model predicts JTX performance reasonably well. The same logic was used in another computer program for predicting the performance of nitrogen J-T cryostats. The predicted flow rate agreed very well with measured flow rates at the normal operating points. These nitrogen cryostats were part of a production order where each unit has its expander capillary tube "calibrated" by clipping off and running a flow test. At first, predictions of required capillary tube length were low by a factor of two. After measuring the inside diameter of a sample of the capillary tubing (same tubing as used for the small capillary in JTX No. 2), the computer predictions based on the measured diameter fell within the measured flow rates at the actual tube lengths used. Figure 3-3 presents the results of this capillary tube study.

The service subroutines which read and perform interpolation of the helium thermophysical properties are all quite specialized. The helium data are restricted to the pressure and temperature ranges within which the JTX is typically expected to operate. The lookup options are controlled by the particular subroutine calling the lookup subroutine. Table 3-1 presents a brief description of the helium properties subroutines and their limitations. A complete tabulation of the thermophysical properties used in the program is given in Appendix B.

A sample printout of the JTX performance prediction program is presented in Figure 3-4. The format is identical for each case, regardless of the number of input changes made. All input parameters are printed out for each case. "Design Parameters" gives the geometrical input, and heat leak, if known; and "Input Conditions" gives the three state points required to define the operating conditions of the case. Every attempt was made to give self-descriptive parameter names. The cycle state point identification numbers refer to those given in Figure 3-1.



S-11019

Figure 3-3. Nitrogen J-T Cryostat Capillary Tube Study

TABLE 3-1

DESCRIPTION OF HELIUM PROPERTIES ROUTINES

Name	Description
HELIUM/DATA	<p>Data element containing helium single-phase properties as a function of temperature and pressure. The temperature range is 2.222-20 K (4.0-36 R). The pressure ranges are as follows:</p> <p>Specific enthalpy 0-20.41 atm (0-300 psia)</p> <p>Specific volume and dynamic viscosity 0.068-20.41 atm (1-300 psia)</p> <p>Thermal conductivity 2.244-20.41 atm (32.99-300 psia)</p>
HEREAD	Reads in helium single-phase thermophysical properties from data element HELIUM/DATA, and converts data arrays to MAPRDY format.
SATPRP	<p>Helium saturation properties lookup by linear interpolation. Contains 41-point data for specific enthalpy, specific volume, and dynamic viscosity from 0.833 K (1.5 R), taken as zero pressure, to the critical point 5.202 K (9.363 R), including the lambda point 2.177 K (3.919 R). Saturated liquid and vapor properties and saturation pressure are given at each temperature. Saturated liquid viscosity below the lambda point (He II) is given as infinitesimally small number since it is not used in program. Four lookup options:</p> <ol style="list-style-type: none"> (1) Pressure in, sat. liquid props. out (2) Pressure in, sat. vapor props. out (3) Enthalpy in, sat. liquid props. out (4) Temperature in, sat. liquid props. out
THERMO	<p>Three-dimensional lookup of helium single-phase specific enthalpy and specific volume read into MAIN program by subroutine HEREAD. Uses MAPRDY for 3-D lookups. Calls SATPRP for saturation data when input P and T fall between single-phase data point and two-phase dome. Linear interpolation then employed. Two lookup options:</p> <ol style="list-style-type: none"> (1) Pressure and temperature in, enthalpy and specific volume out (2) Pressure and enthalpy in, temperature and specific volume out

TABLE 3-1 (Cont)

Name	Description
THERMO (Cont)	With option (2), if pressure is less than critical and enthalpy puts lookup point just outside dome, then it must be on liquid side only. (This only occurs in EXPDR, which must have inlet enthalpy less than critical or He II may not be produced). Low-pressure specific volume (below 1.0 psia) is calculated from ideal gas equation. Specific volume data below critical pressure in single-phase region is limited to liquid side, also.
TRANSP	Three-dimensional lookup of helium single-phase viscosity and thermal conductivity read into MAIN program by subroutine HEREAD. Uses MAPRDY for 3-D lookups. Viscosity P-T lookups below critical pressure performed as in THERMO, being limited to liquid side. Thermal conductivity P-T lookups limited to supercritical pressure (HEATX is the only subroutine using thermal conductivity, and J-T heat exchanger does not operate in intermediate pressure region). All other pressures (below critical) use temperature-dependent built-in data and linear interpolation, since low-pressure transport properties are nearly independent of pressure.
LAGIN2	Performs linear interpolation and extrapolation of any tabular data, using the binary search method of reaching the two data points between which the answer lies (very fast).
MAPRDY	Three-dimensional lookup routine used by THERMO and TRANSP to find properties as a function of two input variables.
KFIN	Data and lookup routine (linear interpolation) for stainless steel tubing and OFHC copper fins. Built-in data provided for temperatures up to 50 K (90 R).

HELIUM-III JOULE-THOMSON EXPANDER AND HEAT EXCHANGER (JTX) PERFORMANCE

DESIGN PARAMETERS

HEAT EXCHANGER GEOMETRY

H=P TUBE I.D. .0120 IN
H=P TUBE O.D. .0220 IN
FIN O.D. .0490 IN
MANDREL O.D. .2000 IN
COIL C-C DIA. .2490 IN
SHEATH I.D. .3100 IN
FIN THICKNESS .0041 IN
FIN PITCH .0099 IN
TUBE LENGTH 15.750 IN

EXPANSION TUBE GEOMETRY

TUBE 1 I.D. .0025 IN
TUBE 2 I.D. .0070 IN
COIL C-C DIA. .2100 IN
TUBE 1 LENGTH 2.900 IN
TUBE 2 LENGTH 8.500 IN
TUBE 1 D-FACTOR 1.0000

ZETA-FACTOR = .750

HEAT LEAK = .00050 WATTS

INPUT CONDITIONS

HIGH-PRESSURE-SIDE INLET TEMPERATURE, T1 = 15.20 K (27.36 R)
HIGH-PRESSURE-SIDE INLET PRESSURE, P1 = 6.805 ATM (100.00 PSIA)
REFRIGERATION TEMPERATURE, T3 = T4 = 1.84 K

CYCLE STATE POINTS

POINT	PRESSURE	TEMPERATURE	ENTHALPY
(1)	6.805 ATM (100.00 PSIA)	15.20 K (27.36 R)	37.486 BTU/LB
(2)	6.741 ATM (99.06 PSIA)	5.79 K (10.41 R)	8.162 BTU/LB
(3L)	.0189 ATM (14.33 TORR)	1.84 K (3.31 R)	.384 BTU/LB
(4)	.0189 ATM (14.33 TORR)	1.84 K (3.31 R)	10.368 BTU/LB
(5)	.0172 ATM (13.05 TORR)	14.93 K (26.87 R)	39.712 BTU/LB

PERFORMANCE SUMMARY

MASS FRACTION LIQUID = .2225 VOLUME FRACTION LIQUID = .0000
MASS FLOW RATE = .3975 GM/MIN (.05258 LB/HR)
NET COOLING LOAD = .03377 WATTS
H.X. EFFICIENCY = 97.97 PERCENT JTX EFFICIENCY = 98.54 PERCENT

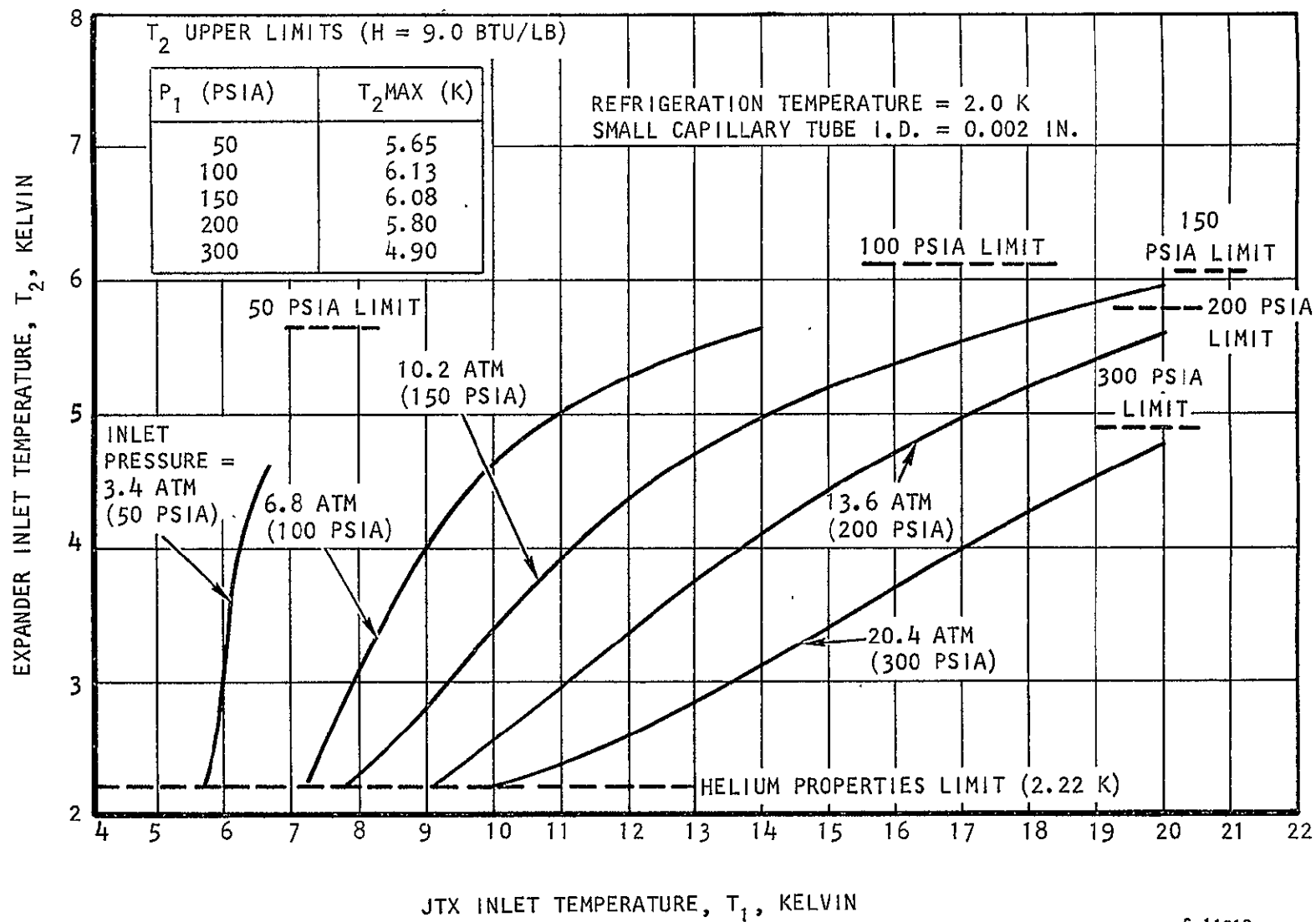
Figure 3-4. Sample Computer Printout of JTX Performance Prediction

JTX NO. 1 PERFORMANCE PREDICTION

The computer program was used to predict the performance of JTX No. 1 over a wide range of inlet temperature and pressure, for the design parameters given in Figure 3-4, with one exception. At the time these predictions were made, the inside diameter of expansion capillary tube No. 1 had not been measured, thus the nominal value of 0.0508 mm (0.002 in.) was used. Five inlet pressures ranging from 3.4 atm (50 psia) to 20.4 atm (300 psia) were studied for a refrigeration load temperature of 2.0 K. After more than 50 runs were made, the range of inlet temperature over which the JTX would produce liquid He II became quite clear. The temperature limits of operation are best illustrated on a plot of expander inlet temperature (T_2 in Figure 3-1) versus JTX inlet temperature (T_1 in Figure 3-1), as shown in Figure 3-5. The lower limit of JTX inlet temperature is not a physical limit, rather a helium properties limit in the computer program. The program has no enthalpy, density, or viscosity data at high pressure (above saturation) below a temperature of 2.22 K (just above lower lambda point), thus preventing characterization of the expander pressure drop and flow rate. No data for He II in this region could be found. The upper limit of expander inlet temperature is based on a value of specific enthalpy just below the critical-point value. Examination of the pressure-enthalpy diagram presented in Appendix B shows that a slightly higher enthalpy value may allow He II production at 2 K, although lower temperature refrigeration would be limited. Even at the critical-point enthalpy the amount of liquid produced at 2 K is very small (about 16 percent, by weight). Other factors considered in this choice of expander specific enthalpy limit are: (1) the uncertainty in the pressure-enthalpy diagram for He II, and (2) the possibility of difficulty in obtaining continuous values of fluid properties when interpolating on data near the critical point (this difficulty is probably the major cause of not obtaining convergence in the expander pressure-drop/flow rate iteration with the present enthalpy limit).

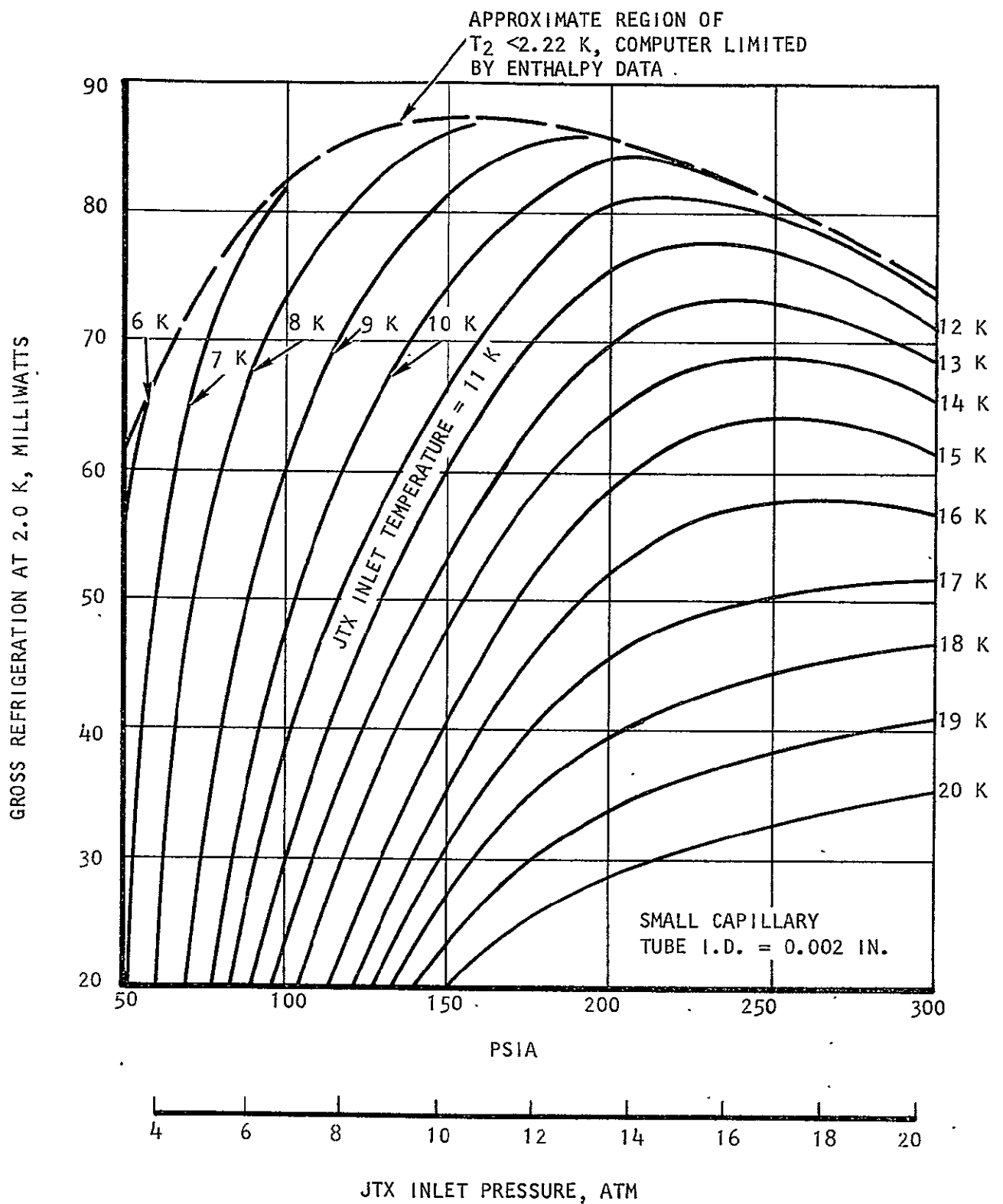
The upper limit of JTX inlet temperature cannot be determined precisely because a heat exchanger effectiveness of exactly 100 percent will not converge in the program. The curves for 3.4 atm (50 psia) and 6.8 atm (100 psia) are stopped at inlet temperatures which gave heat exchanger efficiencies of 99.8 and 99.2 percent, respectively. At the other three pressures the heat exchanger efficiencies were 98.3 percent, or less, at the JTX inlet temperature of 20 K. The JTX will no doubt operate at temperatures above this, although at greatly reduced refrigeration capacity. The 20 K limit is the upper limit of helium properties built into the computer program.

Figure 3-6 shows the predicted gross refrigeration at 2.0 K as a function of JTX inlet pressure and temperature. Note the reduction of cooling capacity as the inlet temperature is increased for a given inlet pressure. At a given inlet temperature, however, there appears to be an "optimum" pressure above and below which the refrigeration capacity drops off. The curves in Figure 3-6 should be considered as approximate, since "smoothing" of many isotherms was required to fill out the plot, especially at the lower temperature and pressures, where very few computer cases actually converged.



S-11018

Figure 3-5. Prediction of JTX No. 1 Expander Inlet Temperature



S-11017

Figure 3-6. Prediction of JTX No. 1 Refrigeration Performance

The best predictions were made in the region above 6.8 atm (100 psia) and 9-10 K. The dashed curve at the top of Figure 3-6 shows the approximate limit set by a minimum allowable expander inlet temperature of 2.22 K, due to lack of high-pressure He II data.

The predicted flow rates for JTX No. 1 as a function of inlet temperature and pressure are presented in Figure 3-7; again, the nominal inside diameter of the small capillary tube was used. The same computer runs produced the data for all three plots (Figures 3-5, 3-6, 3-7). Note that in Figure 3-7 as JTX inlet pressure is increased, the flow rate becomes nearly independent of inlet temperature. This is probably due to the effect of more uniform thermophysical properties as more of the expander operates away from the critical point.

JTX NO. 1 TEST DATA ANALYSIS

In December 1975, the Jet Propulsion Laboratory (JPL) performed tests on JTX No. 1, wherein the assembly shown in Figure 2-4 (with a vacuum container housing the portion below the instrumentation flange) was immersed in a liquid helium dewar. The inlet heater allowed the warmup of a pressurized (liquid) helium stream to the desired JTX inlet temperature.

The preliminary test results (steady-state data) are presented in Table 3-2, as reported by Dr. L. C. Yang.

TABLE 3-2
PRELIMINARY TEST RESULTS OF JTX NO. 1 BY JPL

JTX Inlet Pressure (psia)	JTX Inlet Temperature (K)	Sensor Plate Temperature (K)	Warm-End Sheath Temperature (K)	Mass Flow Rate (lb/hr)	Gross Refrigeration (mW)
100	4.4	1.81	5.0	0.0544	176.8
100	6.6	1.81	6.2	0.0488	150.2
100	10.1	1.85	8.3	0.0528	95.4
100	12.1	1.84	8.6	0.0532	51.5
100	15.2	1.84	11.0	0.0520	25.2
200	4.5	1.9	5.4	0.0808	272.6

It was generally agreed that the demonstration of achieving refrigeration at superfluid He II temperatures, in a stable manner, with a J-T cryostat was a great success. However, evaluation of the counterflow heat exchanger efficiency was impossible because the warm-end sheath temperature apparently did not measure the low-pressure-side outlet gas temperature (T_5 in the schematic of Figure 3-1) well enough. If the values presented in Table 3-2 were used to

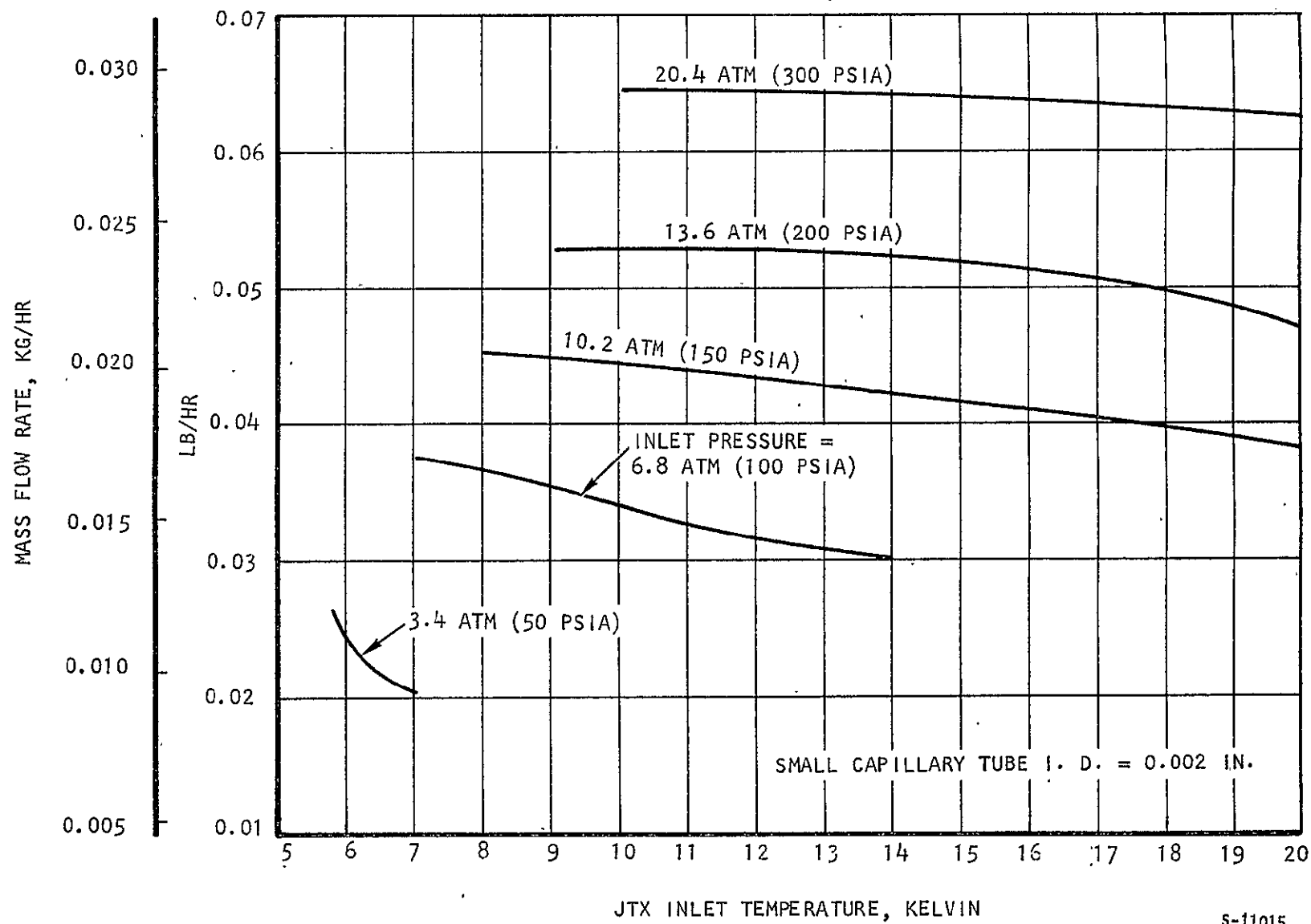


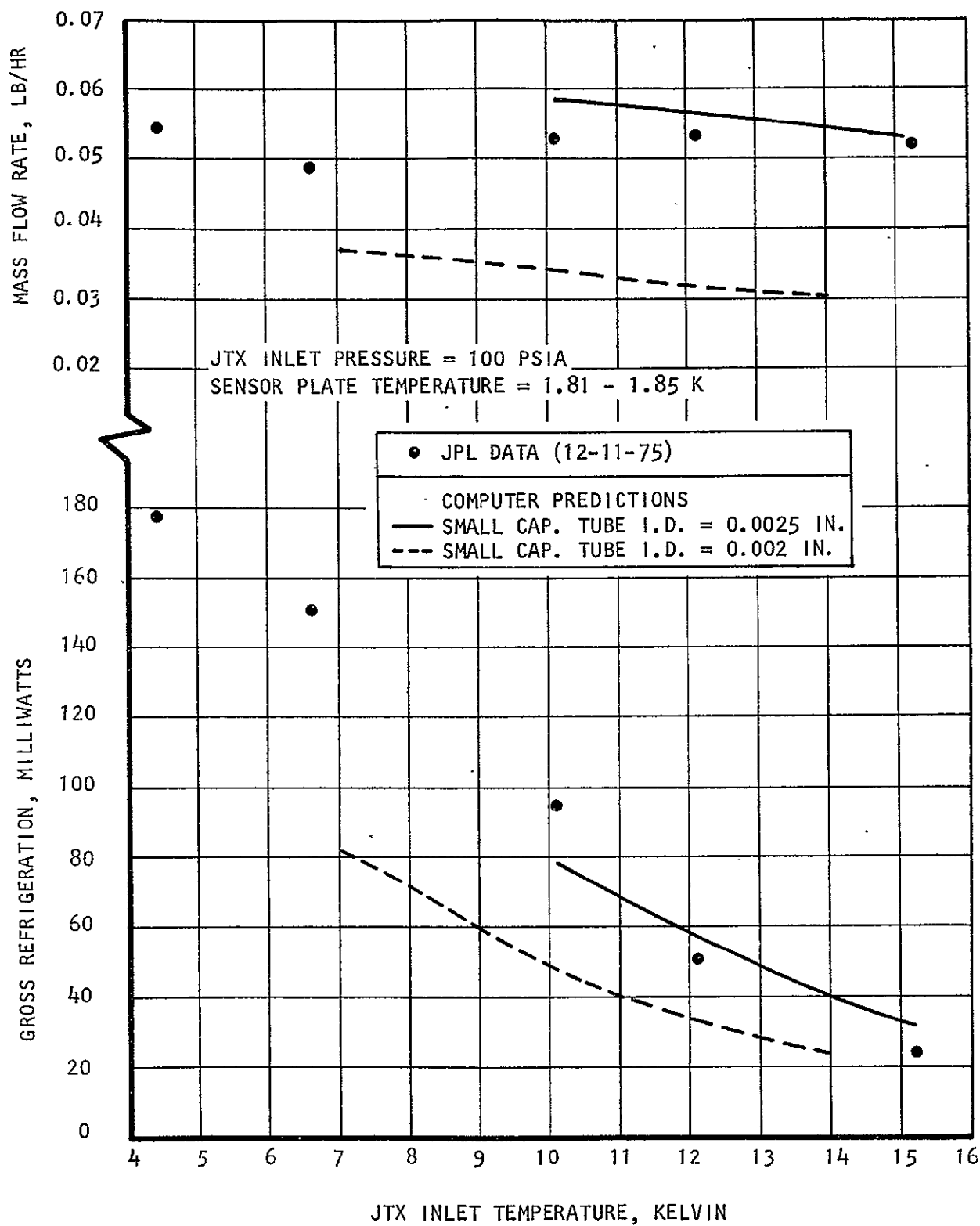
Figure 3-7. Predicted Flow Rate for JTX No. 1

represent T_5 in the thermodynamic cycle analysis, no heat balances around the system are obtained, and for the first and last cases a heat exchanger effectiveness of over 100 percent is indicated. A simplified analysis of the heat transfer from the outlet gas to the sheath near the warm-end sheath temperature measurement, for the third case in Table 3-2, showed that the flowing gas could be 1.7 K warmer than the sheath at that point (8.3 K). This difference is enough to invalidate the heat balance, and prevents a meaningful comparison with the predicted heat exchanger effectiveness (that is 98 percent, versus 78 percent from the 8.3 K data point).

The refrigeration and flow rate data, however, can be made to compare reasonably well with computer program predictions. Figure 3-8 presents a plot of the 100-psia test data, showing gross refrigeration and mass flow rate plotted as a function of JTX inlet temperature. The dashed lines are the predictions based on the nominal inside diameter of the small capillary tube (0.002 in.). The dashed flow rate curve is taken directly from Figure 3-7. The corresponding refrigeration curve is taken from the computer results which were used to construct the performance map of Figure 3-6, hence do not agree exactly with the "smoothed" curves, especially at the higher inlet temperatures. The computer results all used 2.0 K as the refrigeration temperature, rather than the 1.81-1.85 K obtained during testing. The effect of this difference is expected to be very small, however, as the thermophysical properties of helium do not vary significantly between these temperature levels (the only significant effect would be in the heat exchanger low-pressure-side pressure drop, which was not independently evaluated).

Figure 3-8 shows that the measurements of both refrigeration and flow rate were higher than the predicted curves using the nominal capillary tube diameter. As noted in Section 2 of this report, the small capillary tube size was later measured to be 20 to 30 percent larger in diameter (at one point, anyway) than its nominal value. Therefore, new computer predictions were made, using a 25 percent larger inside diameter, and a comparison with the test data showed much better agreement. This is illustrated in Figure 3-8 by the solid-line curves, which appear to be within experimental uncertainty of the test data. The lower inlet-temperature test cases cannot be analyzed by the computer model because of the low-temperature, high-pressure, He II thermophysical properties limitations discussed previously. The lowest temperature tested is lower than the JTX is likely to ever encounter from an actual supercritical helium storage tank. Thus, the low-temperature expander inlet temperature limitation of the computer program is not considered to be a very serious shortcoming.

A performance prediction of JTX No. 1A (same as JTX No. 1 except for a longer, larger diameter, small capillary tube) was made for the third case conditions of Table 3-2, namely, the case of 10.1 K inlet temperature at 100 psia. The results for a refrigeration temperature of 2.0 K were: mass flow rate, 0.0177 kg/hr (0.039 lb/hr); and gross refrigeration, 55 milliwatts. A glance at the nitrogen flow calibration test data of Figure 2-5 reveals a large difference in the predicted flow rate at He II levels as compared with room-temperature nitrogen data. The ratio of JTX No. 1 flow to JTX No. 1A flow



S-11014

Figure 3-8. JTX No. 1 Test Data Comparison with Computer Predictions

at the 2.0 K level is predicted to be 1.50, while the same ratio from the nitrogen room-temperature data is about 4.4. This apparent conflict remains unexplained at this time. No other data exists to substantiate the indication that room-temperature flow data cannot be correlated to He II flow data, as was expected.

JTX NO. 2 PERFORMANCE PREDICTION

The preliminary analysis of JTX No. 2 performance was based on the original design intent -- that is, the same as JTX No. 1 except for doubling the length of the small capillary tube. This was done, over a narrower range of input parameters (27 cases) than for JTX No. 1, before it was established that the small diameter tubing was no longer available. The next larger size tubing was incorporated after estimating how much coiled length of it would fit on the existing mandrel. This length was estimated to be 86 cm (34 in.), assuming a double wrap of 25 coils, followed by 17 coils (12 in.) of the larger (0.018 in. O.D.) capillary tube. The performance prediction computer program was run for these dimensions and the same inlet conditions as several of the JPL test cases. Table 3-3 presents the flow rate results, showing also the predicted values for the capillary tube size originally intended for JTX No. 2 (with a 20 percent increased inside diameter over the nominal size). Although many of these cases were unconverged, the predicted flow rate is probably with 5 to 10 percent of the converged value. The conclusion reached here was to expect the JTX No. 2 flow rate to be approximately the same as the JTX No. 1 test data. Again, as noted above for the case of JTX No. 1A, the He II predicted flow performance is at odds with the room-temperature nitrogen flow calibration test data presented in Figure 2-5.

TABLE 3-3

JTX NO. 2 PREDICTED FLOW RATE
FOR 1.84 K REFRIGERATION (100 PSIA CASES)

JTX Inlet Temperature (K)	Predicted Flow Rate (lb/hr)			JPL Test Flow Rate (lb/hr)
	0.0024 in. I.D. 2.9 in. long cap. tube	0.0024 in. I.D. 5.8 in. long cap. tube	0.004 in. I.D. 34 in. long cap. tube	
10.1	0.0530	0.0388*	0.0552*	0.0528
12.1	0.0511	0.0335	0.0520*	0.0532
15.2	0.0490*	0.0331	0.0485*	0.0520

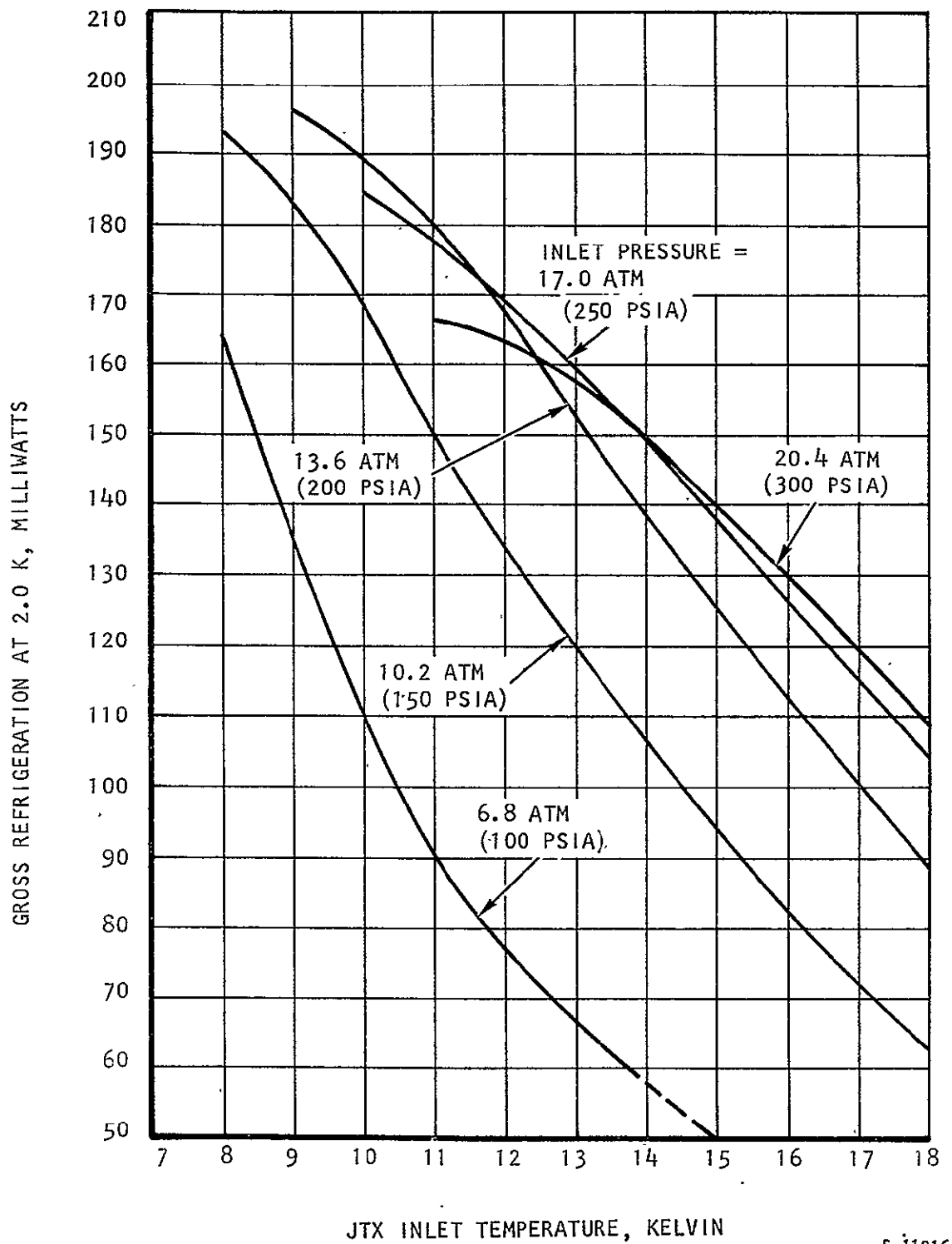
*Unconverged results, due to expander pressure-drop/flow rate problem;
flow rate probably within 5-10 percent of correct value.

JTX NO. 3 PERFORMANCE PREDICTION

The performance prediction of JTX No. 3 was carried out in the same manner as for JTX No. 1. A total of 48 computer cases were run covering 5 values of inlet pressure from 6.8 atm (100 psia) to 20.4 atm (300 psia) and JTX inlet temperatures up to 18 K. The selection of the design points and the range of performance parameters studied is discussed in Reference 1.

All results of the computer runs (except for cases outside the minimum expander inlet temperature limit) were first plotted as gross refrigeration against JTX inlet temperature, for each of the 5 pressures. Unconverged results were plotted along with the converged values, and taken into consideration when drawing the curves, presented in Figure 3-9. Fortunately, the percentage of unconverged results was much smaller over the range of pressures and temperatures studied for JTX No. 3. The expander subroutine seems to work better at higher flow rates.

To obtain a better picture of JTX performance as a function of inlet pressure, the curves of Figure 3-9 are cross-plotted to obtain the refrigeration performance map in Figure 3-10. The corresponding predicted flow rates, as a function of inlet pressure and temperature, are plotted in Figure 3-11, showing the relatively weak dependence on temperature and strong dependence on inlet pressure. Both of these figures are reproduced from Reference 1.



S-11016

Figure 3-9. Predicted JTX No. 3 Refrigeration as a Function of Inlet Temperature

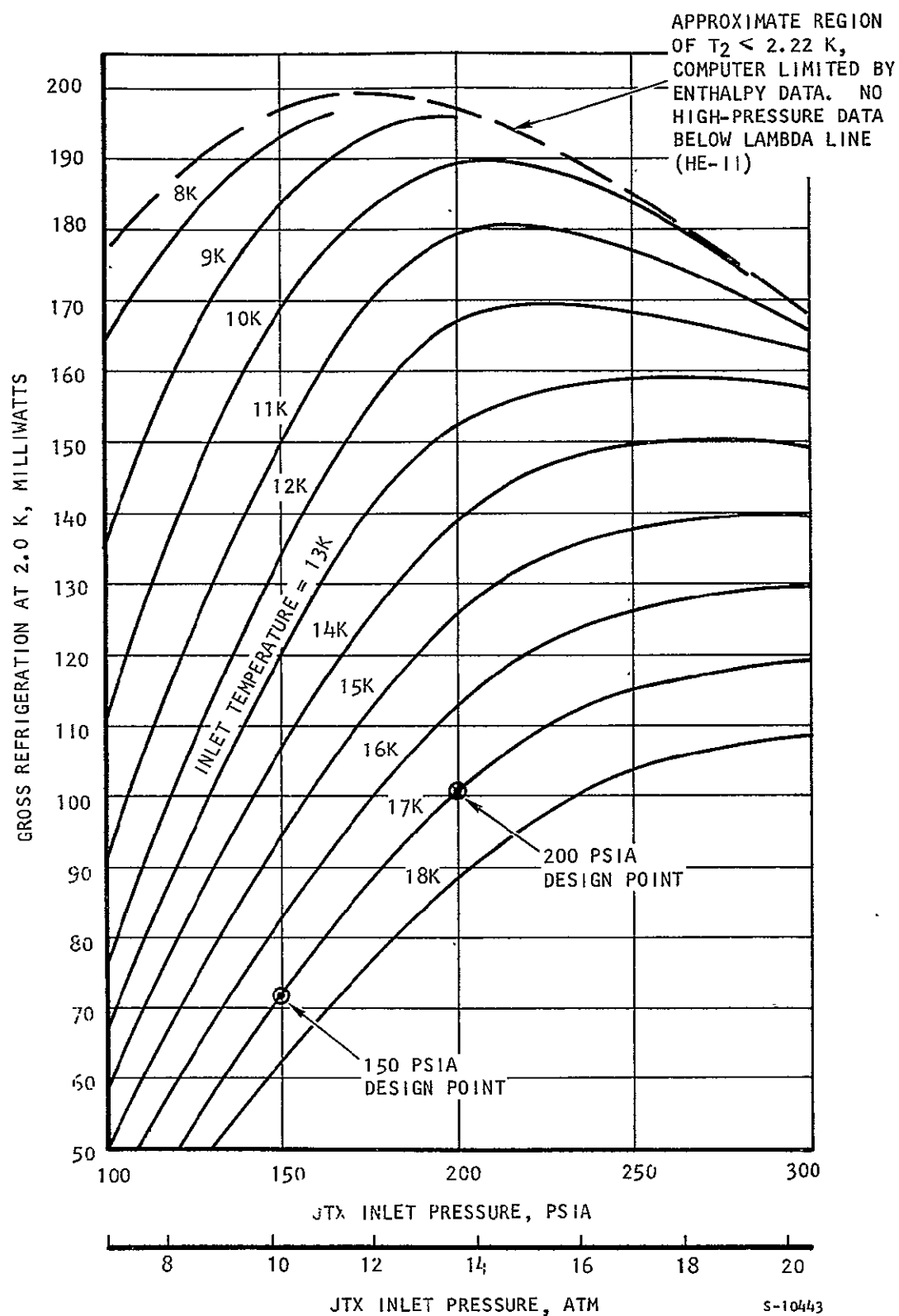


Figure 3-10. Prediction of JTX No. 3 Refrigeration Performance

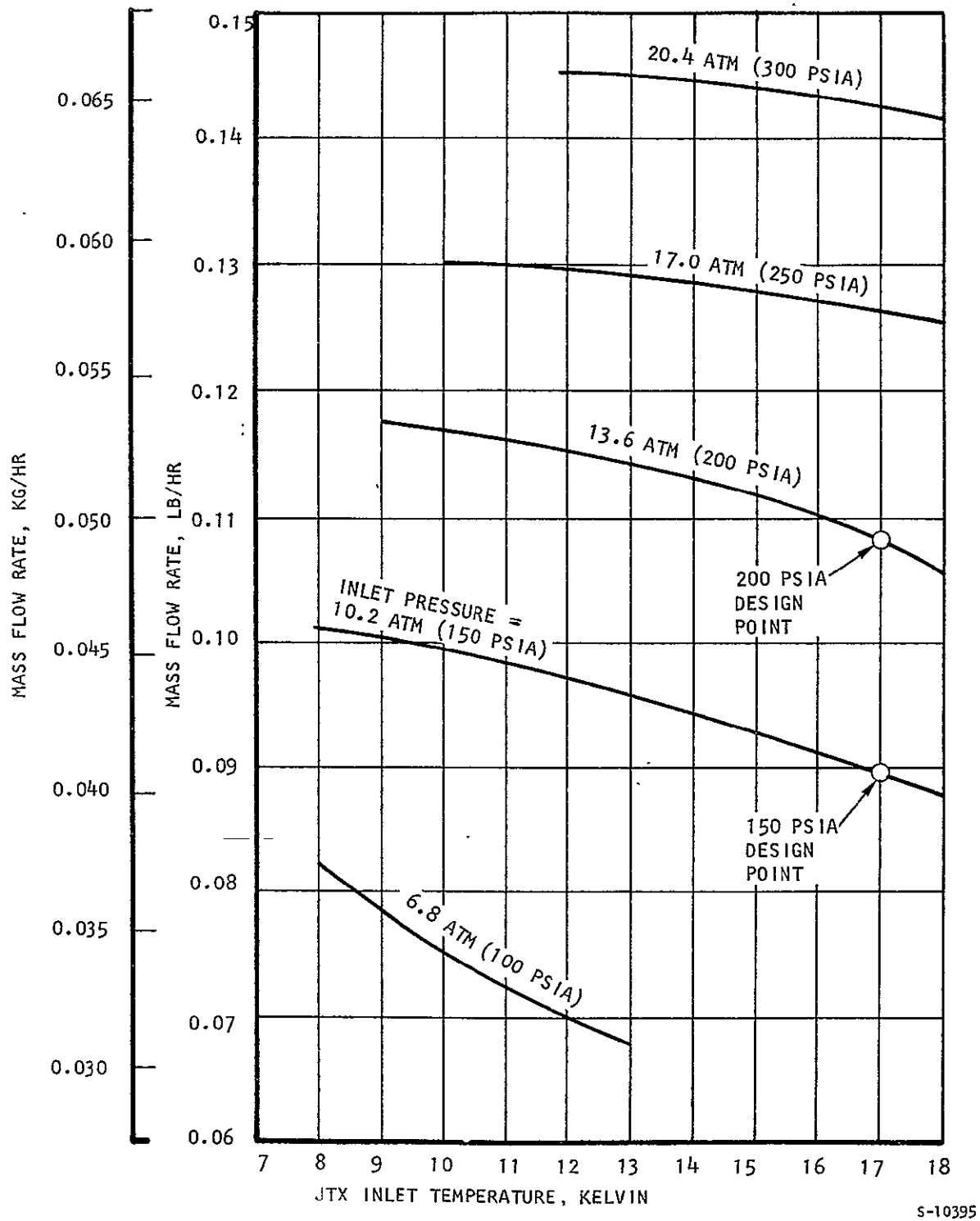


Figure 3-11. Predicted Flow Rates for JTX No. 3

REFERENCES

1. "Preliminary Design Study, Astronomical Detector Cooling System", NASA Contract NAS2-8984, Amendment No. 1, AiResearch Report No. 76-13280, November 17, 1976.
2. Ito, H., "Friction Factors for Turbulent Flow in Curved Pipes," ASME Trans Ser. D, Journal of Basic Engineering, Vol. 81, June 1959, pp 123-134.
3. Kays, W.M. and A. L. London, Compact Heat Exchangers, 2nd Ed., McGraw-Hill, 1964, p. 221.
4. Seban, R. A. and E. F. McLaughlin, "Heat Transfer in Tube Coils with Laminar and Turbulent Flow", International Journal of Heat Mass Transfer, Vol. 6, 1963, pp. 387-395.
5. McCarty, R.D., "Thermophysical Properties of Helium-4 from 4 to 3000 R with Pressures to 15000 PSIA", NBS Technical Note 622, National Bureau of Standards, September 1972.
6. Cook, G.A., ed., Argon, Helium and the Rare Gases, Vol. 1, Interscience Publishers, Inc., New York, 1961, pp. 324, 344, 347-348.
7. Gorter, C. J. ed., Progress in Low Temperature Physics, Vol. II, North-Holland Publishing Co., Amsterdam, 1957, p. 459.
8. Brooks, J.S., The Properties of Superfluid Helium Below 1.6 Kelvin, University of Oregon Ph. D. Thesis, 73-28581, University Microfilms, Ann Arbor, Michigan, June 1973.

APPENDIX A
COMPUTER PROGRAM

NOMENCLATURE

A_f	Flow cross-sectional area
A_{fs}	Fin surface area
A_i	Surface area inside high-pressure tube
A_o	Finned tube surface area on low-pressure side
A_s	Total surface area on low-pressure side
C	Capacity rate ratio = C_{MIN}/C_{MAX}
C_{MAX}	Maximum of C_{PH} and C_{PL}
C_{MIN}	Minimum of C_{PH} and C_{PL}
C_{PH}	Heat capacity, high-pressure side
C_{PL}	Heat capacity, low-pressure side
D_c	Finned tube coil diameter
D_{ec}	Expander tube coil diameter
D_{e1}	Inside diameter of small expander tube
D_{e2}	Inside diameter of large expander tube
D_f	Finned tube overall diameter
D_h	Hydraulic diameter
D_i	High-pressure tube inside diameter
D_m	Mandrel outside diameter
D_o	High-pressure tube outside diameter
D_s	Sheath inside diameter
DPV	Volume-normalized low-pressure side pressure drop
f_{ei}	Friction factor (Darcy) in expander tube increment
f_i	Friction factor (Darcy) inside high-pressure tube
f_o	Friction factor (Fanning) outside finned tube

G	Mass velocity = W/A_f
g_c	Constant = 4.1698×10^8
H	Specific enthalpy
h_i	Heat transfer coefficient inside high-pressure tube
h_o	Heat transfer coefficient outside finned tube
k	Thermal conductivity
K_E	Expansion loss factor between expander tubes
L_{e1}	Length of small expander tube
L_{e2}	Length of large expander tube
L_T	Total length of finned tube
L_x	Increment length of expander tube
ML_f	Fin efficiency parameter
N_{tu}	Number of transfer units = $UA/(W \cdot C_{MIN})$
P	Absolute pressure
p	Fin pitch
P_{ex}	Expander exit pressure
Pr	Prandtl number = $C_p \mu / k$
ΔP_i	Pressure drop inside high-pressure tube
ΔP_o	Pressure drop outside finned tube
ΔP_x	Expander pressure drop
Q	Refrigeration capacity or heat leak
Re	Reynolds number = $D_h G / \mu$
T	Absolute temperature
UA	Overall heat exchanger conductance
V	Specific volume
W	Mass flow rate

X_L	Mass fraction liquid
Y_L	Volume fraction liquid
Z	Zeta-factor, flow restriction factor for nylon fin seals

Greek

δ	Fin thickness
ϵ_{HX}	Heat exchanger effectiveness
η_f	Fin surface efficiency
η_o	Overall finned-tube surface efficiency
μ	Dynamic viscosity

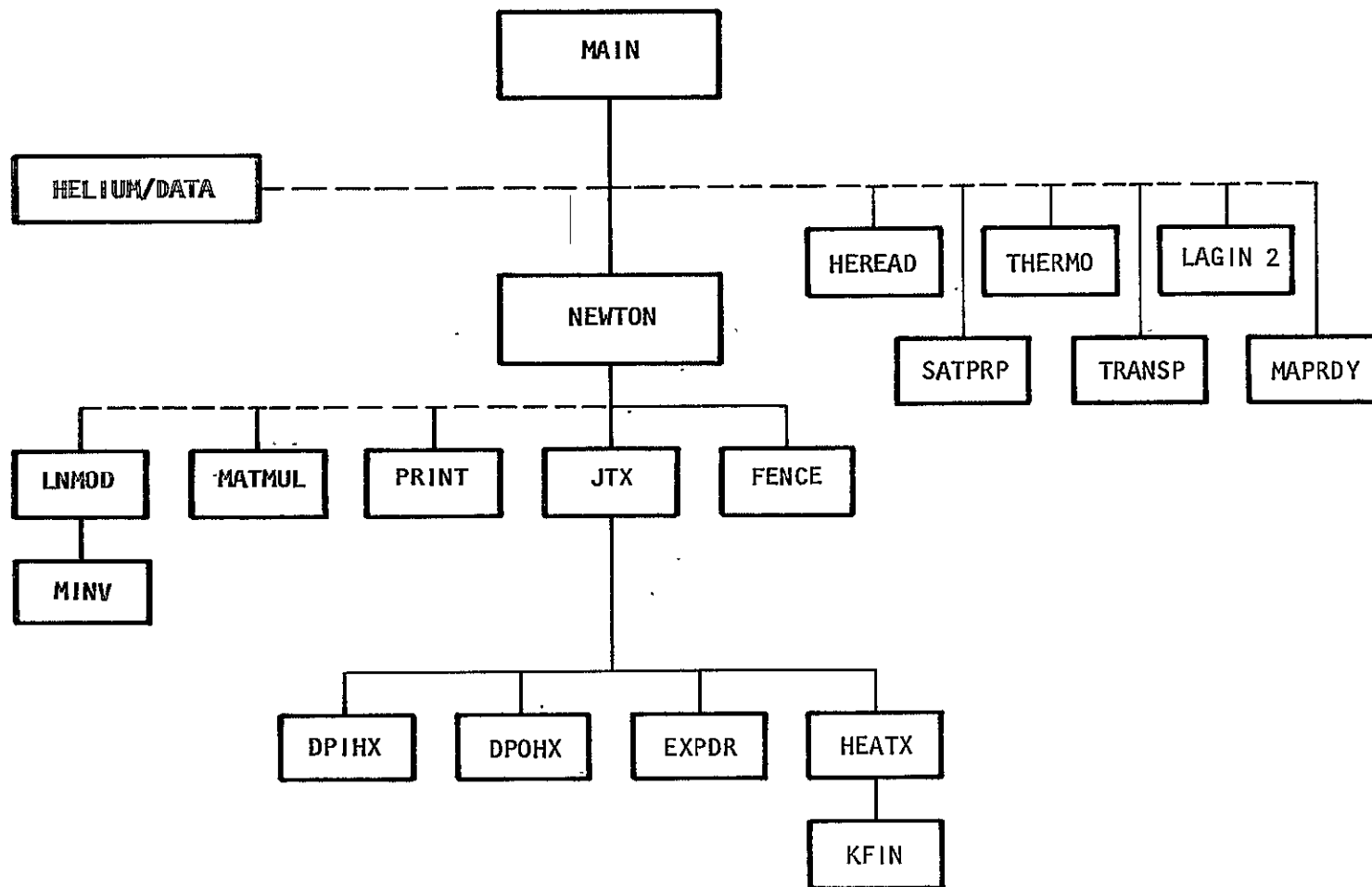


Figure A-1. JTX Computer Program Subroutine Structure

S-11013

MAIN PROGRAM

Call **HEREAD**

Reads "Helium/Data" H, V, μ , k vs P, T;

Program internal units are PSIA, $^{\circ}\text{R}$, BTU, LB, FT, HR

Read Geometrical Input (inches), Q_{LEAK} (Watts), Z (ZETA-Factor)

Read Input Conditions:

$$T_1, P_1, T_3$$

Make Initial Guesses

$$T_2 = T_{2\text{MIN}} = 2.222\text{K} (4.0^{\circ}\text{R})$$

$$W = 2.722 \times 10^5 \left[\left(\frac{D_{e1}}{12} \right)^5 \left(\Delta P_x \right) / \left(f_x L_{e1} \bar{V} / 12 \right) \right]^{1/2} = \text{LB/HR}$$

$$\text{where } \Delta P_x = P_1$$

$$f_x = 0.025$$

$$\bar{V} = (V_2 + V_L) / 2, V_2 = f(P_1, T_2)$$

$$V_L = f(H_2, \text{SAT.LIQ.})$$

Call **NEWTON** —

Which calls JTX numerous times, gives all cycle points, W, e_{HX}

Calculate:

$$X_L = (H_4 - H_2) / (H_4 - H_{3L})$$

$$Y_L = X_L V_{3L} / [X_L V_{3L} + (1 - X_L) V_{3v}]$$

$$Q_{\text{TOT}} = W(H_5 - H_1) / 3.41443$$

$$Q_{\text{NET}} = Q_{\text{TOT}} - Q_{\text{LEAK}}$$

$$\eta_{\text{JTX}} = 100 Q_{\text{NET}} / Q_{\text{TOT}} \text{ (Percent)}$$

Write Output

SUBROUTINE JTX; CYCLE ANALYSIS

Call **DPIHX**

$$\Delta P_i = f(P_1, T_1, T_2, W)$$

$$P_2 = P_1 - \Delta P_i$$

Call **EXPDR**

$$\Delta P_x = f(P_2, T_2, W)$$

Call **SATPRP**

$$P_3 = f(T_3)$$

Call **DPOHX**

$$\Delta P_o = f(P_3, T_3, T_5, W)$$

T_5 is approximated by T_1 since T_5 is still unknown

$$P_5 = P_3 - \Delta P_o$$

First convergence closure

$$CLX1 = \left[\text{LOG}_e (\Delta P_x) - \text{LOG}_e (P_2 - P_3) \right] / \text{LOG}_e (P_2 - P_3)$$

Properties Lookups **SATPRP** , **THERMO**

$$T_4 = T_3$$

$$H_4 = f(P_3), (H_4 = H_{3v})$$

$$H_1 = f(P_1, T_1)$$

$$H_2 = f(P_2, T_2)$$

HX Heat Balance

$$H_5 = H_4 + H_1 - H_2$$

Call **THERMO**

$T_5 = f(P_5, H_5)$, If $T_5 \geq T_1$, Set Flag5 = 1.0 for printout later in **MAIN**

SUBROUTINE JTX (Continued)

HX Heat Capacities

$$C_{PH} = (H_1 - H_2)/(T_1 - T_2)$$

$$C_{PL} = (H_5 - H_4)/(T_5 - T_4)$$

$$C_{MIN} = \min(C_{PH}, C_{PL}), C_{MAX} = \max(C_{PH}, C_{PL}), C = C_{MIN}/C_{MAX}$$

Call HEATX

$$UA = f(P_1, T_1, P_2, T_2, P_3, T_3, T_5, W, C_{PH}, C_{PL})$$

HX Effectiveness

$$N_{tu} = UA/(W C_{MIN})$$

$$\epsilon'_{HX} = \left\{ 1 - \exp \left[-N_{tu} (1 - C) \right] \right\} / \left\{ 1 - C \cdot \exp \left[-N_{tu} (1 - C) \right] \right\}$$

$$\text{If } C > .999999, \epsilon'_{HX} = N_{tu}/(1 + N_{tu})$$

$$T'_5 = T_4 + \epsilon'_{HX} (T_1 - T_4) C_{MIN}/C_{PL}$$

$$\text{If } T'_5 \geq T_1, C_{PL} = C_{MIN}$$

$$\epsilon_{HX} = C_{PL} (T'_5 - T_4) / [C_{MIN} (T_1 - T_4)]$$

Second Convergence Closure

$$CLX2 = (T'_5 - T_5)/T_5$$

SUBROUTINE NEWTON; CONVERGENCE CRITERION

Guess T_2 and W in MAIN

Call JTX

To obtain CLX1 and CLX2

Calculate Error Vector

$$ERR = \sqrt{(CLX1)^2 + (CLX2)^2}$$

Test Convergence

If $ERR \leq CONV$, then T_2 and W are okay

$$CONV = 0.005 \text{ (0.5\%)}$$

SUBROUTINE DPIHX ; HIGH-PRESSURE-SIDE (INSIDE TUBE) PRESSURE DROP

Calculate Geometry Parameters (All Dimensions Were Inches)

$$L_{\text{NO-FIN}} = 3.35 \text{ in. (Built in -- accounts for inlet section of tubing upstream of HX.)}$$

$$D_h = D_i / 12$$

$$A_f = \frac{\pi}{4} D_h^2$$

$$G = W/A_f$$

Fluid Properties

TRANSP

$$\mu_1 = f(P_1, T_1)$$

$$\mu_2 = f(P_2, T_2), P_2 \text{ is approximated by } P_1 \text{ since } P_2 \text{ is still unknown}$$

$$\bar{\mu} = (\mu_1 + \mu_2)/2$$

THERMO

$$V_1 = f(P_1, T_1)$$

$$V_2 = f(P_2, T_2)$$

$$\bar{V} = (V_1 + V_2)/2$$

Pressure Drop

$$Re = D_h G / \bar{\mu}$$

$$f_i = 0.029 (D_i/D_c)^{0.5} + 0.304 (Re)^{-0.25}$$

$$\Delta P_i = \left[\frac{f_i (L_T + L_{\text{NO-FIN}})}{D_i} \right] \left[\frac{\bar{V} G^2}{288 g_c} \right] = \text{PSID}$$

SUBROUTINE DPOHX ; LOW-PRESSURE-SIDE (OUTSIDE FINNED TUBE) PRESSURE DROP

Calculate Geometrical Parameters (All Dimensions Were Inches)

$$A_o = \pi L_T \left[D_o \left(1 - \frac{\delta}{p} \right) + \left(D_f^2 / 2p \right) \left(1 - \frac{D_o^2}{D_f^2} \right) \right] \frac{1}{144}$$

$$A_s = A_o + L_T D_f D_s / (144 D_c)$$

$$C_1 = \left(D_s^2 - D_m^2 \right) \quad C_2 = \left(D_o / D_f \right) + \left(1 - \frac{D_o}{D_f} \right) \left(\frac{\delta}{p} \right)$$

SUBROUTINE DPOHX (Continued)

$$C_3 = (D_o/D_f) \left(1 - \frac{\delta}{p}\right) \quad C_4 = (D_f/2p) \left(1 - D_o^2/D_f^2\right)$$

$$D_h = \left[\frac{C_1 - 4D_f D_c C_2}{\pi D_c (C_3 + C_4) + D_s} \right]^{1/2}$$

$$A_f = (\pi C_1/4 - \pi D_f D_c C_2) Z/144 \quad Z = (\text{Zeta-Factor})$$

Flow Restriction Factor for
Nylon Fin Seals

Fluid Properties

SATPRP

$$V_4, \mu_4 = f(P_3) \quad \bar{\mu} = (\mu_4 + \mu_5)/2$$

THERMO

$$V_5 = f(P_3, T_5) \quad \bar{V} = (V_4 + V_5)/2$$

$$\mu_5 = f(P_3, T_5)$$

Pressure Drop

$$Re = D_h G/\bar{\mu} \quad \text{If } Re \leq 1000, f_o = 0.545 (Re)^{-0.340}$$

$$\text{If } Re > 1000, f_o = 0.203 (Re)^{-0.197}$$

$$\text{If } Re \leq 167.4, f_o = 16/Re$$

$$\Delta P_o = \left[\frac{f_o A_s}{A_f} \right] \left[\frac{\bar{V} G^2}{288 g_c} \right] = \text{PSID}$$

Check Outlet Pressure

$$DPV = \Delta P_o / \bar{V}$$

$$P_{5MIN} = 0.001934 \quad (0.10 \text{ TORR})$$

$$P'_5 = P_3 - \Delta P_o$$

If $P'_5 < P_{5MIN}$, $\Delta P_o = P_3 - P_{5MIN}$, RETURN TO JTX. The output value of P_5 will then be "0.10 TORR", signalling that ΔP_o is too large, but program continues.

If $P'_5 \geq P_{5MIN}$, call THERMO $V'_5 = f(P'_5, T_5)$, $\bar{V}' = (V_4 + V'_5)/2$

$$\Delta P'_0 = DPV \cdot \bar{V}'$$

$$P_5 = P_3 - \Delta P'_0$$

At this point an iteration is performed on V'_5 until P'_5 and P_5 are converged (0.5%), or 20 iterations are made, then last $\Delta P'_0$ becomes final answer.

If $P'_5 < P_{5MIN}$ during this iteration, then return to JTX as noted above, and P_5 will be "0.10 TORR".

SUBROUTINE EXPDR ; EXPANDER PRESSURE DROP

Two Capillary Tubes, each Divided into 20 Increments of Length, each Tube Increment Uses Same Equation for ΔP_x

$$Re = D_{ei} G / \mu \quad \text{where } i = 1 \text{ or } 2$$

$$f_e = 0.029 (D_{ei}/D_{ec})^{0.5} + 0.304 (Re)^{-0.25}$$

$$\Delta P_x = \left(\frac{f_e L_x}{D_{ei}} \right) \left(\frac{\bar{V} G^2}{288 g_c} \right) = \text{PSID}$$

Sudden Expansion Loss Between Tubes

$$K_E = \left[1 - \left(\frac{D_{e1}}{D_{e2}} \right)^2 \right]^2$$

$$\Delta P_{1 \rightarrow 2} = K_E \left(\frac{\bar{V} G^2}{288 g_c} \right)$$

Exit Expansion Loss

$$K_{EX} = 1.0 \quad \Delta P_E = \frac{\bar{V} G^2}{288 g_c}$$

Fluid Properties Depend on Increment Inlet Pressure, P_x , and Temperature, T_x ,
Lookups Depend on Pressure Level

THERMO

$$H_2 = f(P_2, T_2)$$

SUBROUTINE EXPDR (Continued)

SATPRP

$$P_{SL} = f(H_2, \text{SAT. LIQ.})$$

$$P_\lambda = 0.730 \text{ PSIA (BUILT IN)}$$

$$\left. \begin{aligned} \text{If } P_x > P_{SL}, \quad \bar{V} &= f(P_x, H_2) \\ T_x &= f(P_x, H_2) \end{aligned} \right\} \quad \text{THERMO}$$

$$\bar{\mu} = f(P_x, T_x) \quad \text{TRANSP}$$

$$\left. \begin{aligned} \text{If } P_\lambda < P_x \leq P_{SL}, \quad H_L, V_L, \mu_L &= f(P_x, \text{SAT. LIQ.}) \\ H_V, V_V, \mu_V &= f(P_x, \text{SAT. VAP.}) \end{aligned} \right\} \quad \text{SATPRP}$$

$$X = (H_2 - H_L) / (H_V - H_L)$$

$$\left. \begin{aligned} \bar{V} &= V_L + X(V_V - V_L) \\ \bar{\mu} &= \mu_L + X(\mu_V - \mu_L) \end{aligned} \right\} \quad \text{Mixed-mean, or Homogenized Properties}$$

$$\text{If } P_x \leq P_\lambda, \quad \bar{V}, \bar{\mu} = f(P_x, \text{SAT. VAP.}) \quad \text{SATPRP}$$

Normal Calculation

$$P_1 = P_2, \quad P_2 = P_1 - \Delta P_1, \quad P_3 = P_2 - \Delta P_2, \quad \text{ETC} \dots, \quad P_n = P_{n-1} - \Delta P_{n-1}$$

$$\text{Exit of section, } P_{n+1} = P_n - \Delta P_n;$$

$$\text{Exit of expander, } P_{ex} = P_{n+1} - \Delta P_{K_E} = 1.0$$

$$\Delta P_x = P_2 - P_{ex}$$

Conditional Calculation

Does not stop program, just assumes W is wrong, **NEWTON** should determine next step. When flow is too high, the exit of any step could give negative pressure. Calculate an extrapolated (to end of line) exit pressure

$$P'_{ex} = P_i - \Delta P_i (L - L_i) / (\Delta L), \quad \text{where } L_i = i(\Delta L)$$

$$\Delta P_x = P_2 - P'_{ex}$$

SUBROUTINE HEATX ; HEAT EXCHANGER OVERALL CONDUCTANCE

Geometrical Parameters same as DPIHX and DPOHX , with addition of:

$$A_i = \pi D_i L_T / 144$$

$$A_{fs} = (\pi L_T / 2\pi) (D_f^2 - D_o^2) / 144$$

Fluid Properties same as DPIHX and DPOHX , with addition of:

$$\overline{Pr} = C_p \overline{\mu} / \overline{k} = f(P_1, T_1, P_2, T_2, P_3, T_3, T_5)$$

Heat Transfer Coefficients

$$\text{Inside tube: } h_i = 0.023 (Re_i)^{0.85} (Pr_i)^{0.4} \left(\frac{D_i}{D_c} \right)^{0.1} \left(\frac{12 \overline{k}}{D_i} \right)$$

$$\text{Outside (Fins): } h_o = 0.221 (Re_o)^{-0.401} C_{PL} G_o (Pr_o)^{-0.6667}$$

Fin Efficiency (Applies to Copper Only)

Call KFIN

$$k_f, k_t = f(\overline{T}), \overline{T} = (T_1 + T_2 + T_3 + T_5) / 4 \quad \text{Subscripts:}$$

f = fin (OFHC CU)
t = tube (STAINLESS)

$$ML_f = \sqrt{\frac{24 h_o}{k_f \delta}} (D_f - D_o) / 24$$

$$\eta_f = \frac{\text{TANH } ML_f}{ML_f} \quad \eta_o = 1 - \left(\frac{A_{fs}}{A_o} \right) (1 - \eta_f)$$

Overall Conductance (BTU/Hr-°R)

$$UA = \left[\frac{1}{h_i A_i} + \frac{\text{LOG}_e (D_o / D_i)}{2\pi L_T k_t / 12} + \frac{1}{\eta_o h_o A_o} \right]^{-1}$$

· APPENDIX B
THERMOPHYSICAL PROPERTIES

APPENDIX B

THERMOPHYSICAL PROPERTIES

DEVELOPMENT OF PRESSURE-ENTHALPY DIAGRAM

Introduction

In order to analyze the performance of a Joule-Thomson expander operating into the helium II (superfluid) region, that is, at temperatures below 2.177 K (saturation pressure of 0.0497 atm), it is most convenient to utilize a pressure-versus-enthalpy (P-H) diagram. Since a diagram of this type could not be found in the literature, one was generated from a recent publication of helium I data (Reference 5), together with several other sources of certain helium II data (References 6, 7, and 8), and some key assumptions. The following paragraphs outline the procedure used to generate the helium P-H Diagram of Figure B-1.

Helium I Above 1.0 Psia

Referring to Figure B-1, all the data above 4.0 R and 1.0 psia are taken directly from McCarty, NBS-TN-622 (Reference 5).

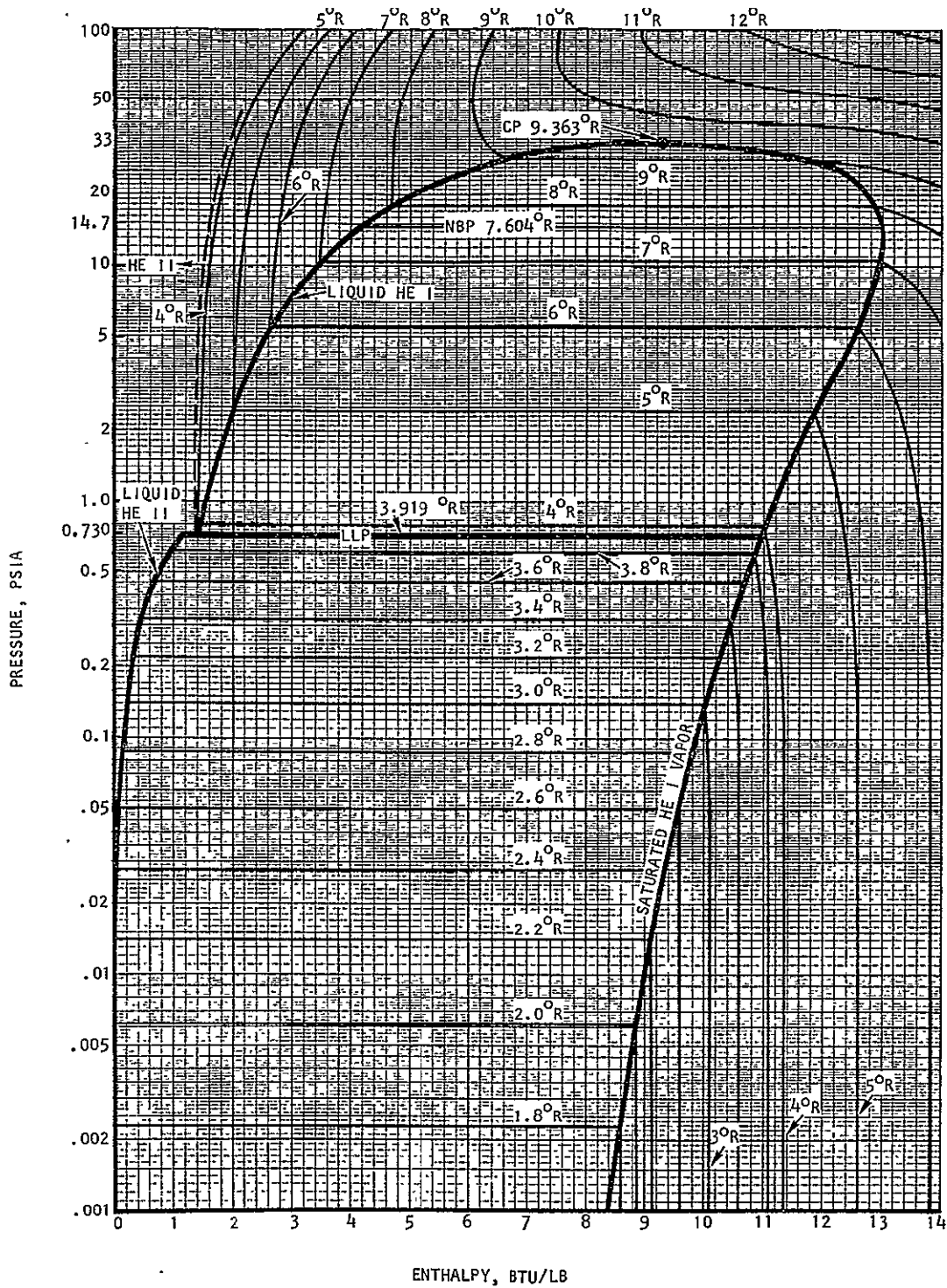
Helium II Coexisting with Vapor

The region below the lower lambda point, "LLP" in Figure B-1, and to the left of the saturated He I vapor line is constructed as follows. The phase (P-T) relationship, plotted in Figure B-2, is taken from Cook, p. 324 (Reference 6), which is based on the NBS 1958 He-4 temperature scale. A preliminary estimate of the liquid He II line was calculated from specific heat (C_s)* data (Cook, p. 344) and the enthalpy equation:

$$H_L = \int_{T_0}^T C_s dT + (P/p) \quad (B-1)$$

where the second term is assumed to be negligible, and $C_s \approx 0$ at $T_0 = 1.5$ R. This probably slightly underestimates C_v (heat capacity at constant volume) for LHe II. Then a preliminary He I vapor line was obtained by adding the latent heat of vaporization (from Cook, p. 348) to H_L . Extrapolating latent heat values from McCarty to 3.919 R (lower lambda point as given by McCarty) showed a 2.3 percent discrepancy with the earlier published data (Cook, p. 348 and Gorter, Reference 7, p. 459; same original source). However, the enthalpy of

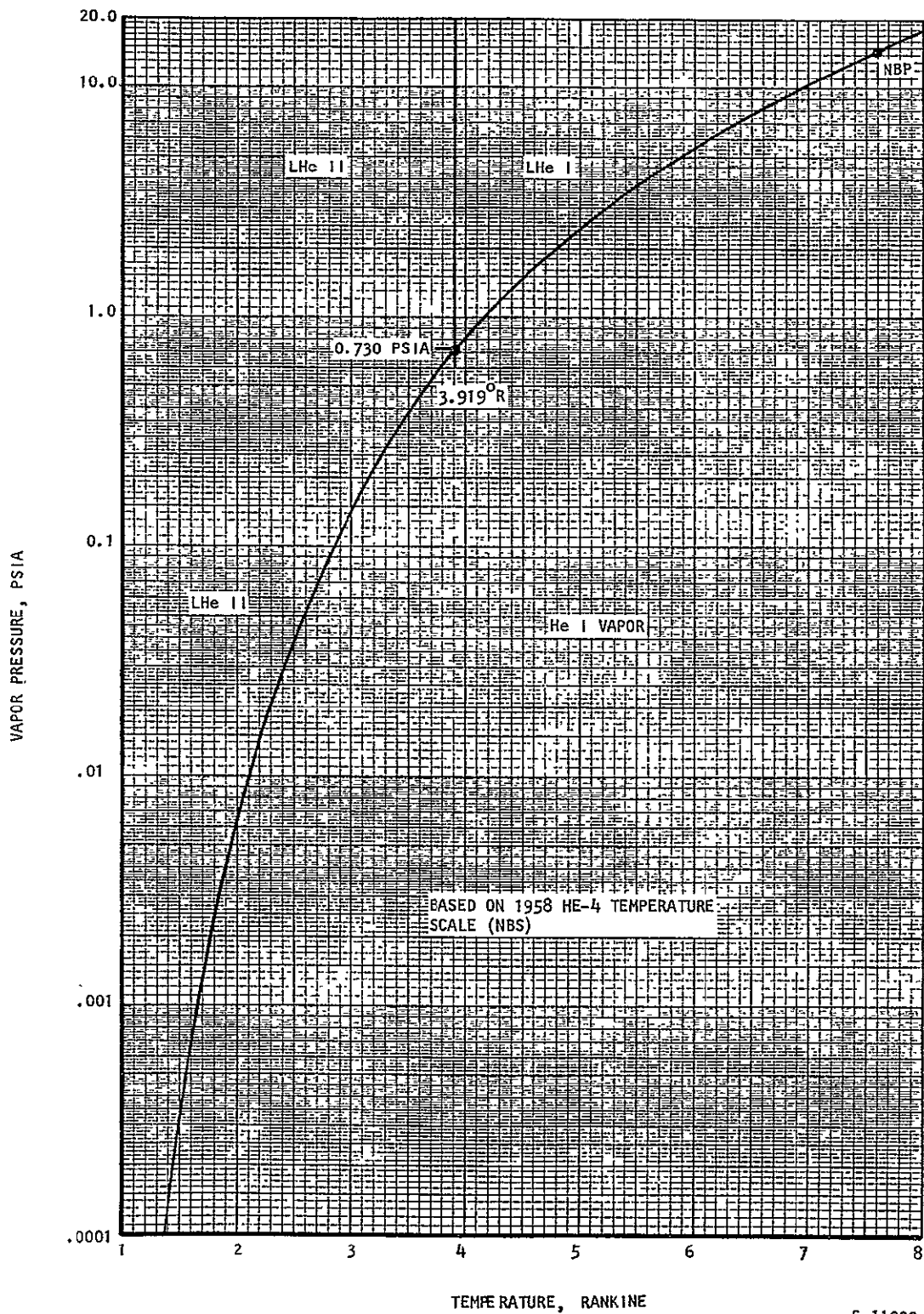
* C_s is the heat capacity measured at the vapor pressure.



S-11023

Figure B-1. Pressure-Enthalpy Diagram for Helium-4 Including Helium II Region

REPRODUCIBILITY OF THE
ORIGINAL PAGE IS POOR



S-11022

Figure B-2. Vapor Pressure of Helium-4 Including Helium II Region

saturated vapor at 3.919 R was only 1.2 percent different. Therefore, the saturated vapor values below the lambda point were adjusted to make a smooth curve with McCarty values above 1.0 psia. Using the latent heat data from Cook and Gorter with this saturated vapor line resulted in a shift of the H curve. The LHe II enthalpy curve immediately below the lambda point is not exactly known (Cook, p. 347). The curve as shown in Figure B-1 near the lambda point largely reflects the difference between the extrapolated McCarty and Cook latent heat of vaporization data, and the sharp peak in the specific heat curve (used in Equation B-1). The liquid He II curve is felt to be reasonable accurate below 3.8 R (approximately 0.6 psia).

Low-Pressure Superheated Vapor

Isotherms below 1.0 psia on the vapor side of the saturation dome are constructed from McCarty's heat capacity data, C_p , extrapolated to the zero pressure (ideal gas) value of 1.241 Btu/lb-R. Then the enthalpy is calculated from

$$H = H_{SV} + \int_{T_s}^T C_p dT \quad (B-2)$$

where H_{SV} is the previously calculated saturated He I vapor enthalpy and T_s is the saturation temperature. Departure from ideal gas behavior is insignificant below about 0.1 psia, hence the isotherms become vertical lines.

TABULATION OF PROPERTIES

The following pages present a complete tabulation of the thermophysical properties of helium used in the JTX computer program, as well as the thermal conductivity for stainless steel and OFHC copper in the temperature range below 50 K.

10.17.15

SATURATION DATA FOR HELIUM, NP= 4-1 POINTS

T (°R)	P (PSIA)	ENTHALPY (BTU/LB)		SPECIFIC VOLUME (FT ³ /LB)		VISCOSITY (10 ⁻⁶ LB/FT-SEC)		T (°R)
		LIQUID	VAPOR	LIQUID	VAPOR	LIQUID	VAPOR	
1.5	0.	0.	8.24	.1103	12600.	.0001	.100	1.5
1.8	.0023	.005	8.60	.1103	2100.	.0001	.131	1.8
2.0	.0062	.012	8.85	.1103	865.	.0001	.152	2.0
2.2	.0142	.026	9.11	.1103	415.	.0001	.173	2.2
2.4	.028	.050	9.35	.1103	230.	.0001	.195	2.4
2.6	.051	.086	9.59	.1102	136.0	.0001	.217	2.6
2.8	.088	.140	9.83	.1102	84.45	.0001	.240	2.8
3.0	.142	.20	10.05	.1101	55.68	.0001	.262	3.0
3.2	.220	.30	10.27	.1101	38.06	.0001	.285	3.2
3.4	.322	.45	10.48	.1100	27.40	.0001	.306	3.4
3.6	.460	.66	10.68	.1099	20.14	.0001	.329	3.6
3.8	.620	.93	10.85	.1098	15.62	.0001	.350	3.8
3.919	.730	1.17	10.93	.1096	13.61	2.40	.361	3.919
4.0	.815	1.440	11.01	.1097	12.40	2.44	.371	4.0
4.2	1.049	1.572	11.20	.1100	10.01	2.48	.394	4.2
4.4	1.325	1.686	11.39	.1104	8.211	2.50	.417	4.4
4.6	1.649	1.794	11.56	.1109	6.821	2.51	.441	4.6
4.8	2.022	1.902	11.73	.1115	5.731	2.51	.464	4.8
5.0	2.450	2.012	11.89	.1121	4.862	2.50	.487	5.0
5.2	2.936	2.128	12.04	.1127	4.162	2.49	.511	5.2
5.4	3.484	2.251	12.19	.1135	3.589	2.47	.535	5.4
5.6	4.097	2.380	12.32	.1143	3.116	2.45	.559	5.6
5.8	4.780	2.516	12.44	.1152	2.721	2.43	.584	5.8
6.0	5.536	2.660	12.55	.1162	2.389	2.40	.609	6.0
6.2	6.368	2.812	12.65	.1172	2.107	2.37	.635	6.2
6.4	7.282	2.974	12.74	.1183	1.865	2.34	.661	6.4
6.6	8.280	3.144	12.82	.1196	1.657	2.31	.688	6.6
6.8	9.365	3.325	12.88	.1210	1.477	2.28	.716	6.8
7.0	10.54	3.517	12.93	.1225	1.320	2.24	.745	7.0
7.2	11.82	3.721	12.96	.1242	1.181	2.21	.774	7.2
7.4	13.19	3.939	12.97	.1260	1.059	2.17	.805	7.4
7.604	14.696	4.178	12.96	.1282	.9484	2.13	.838	7.604
7.8	16.25	4.424	12.93	.1305	.8530	2.09	.871	7.8
8.0	17.95	4.696	12.87	.1332	.7649	2.05	.906	8.0
8.2	19.77	4.992	12.77	.1363	.6845	2.00	.944	8.2
8.4	21.71	5.318	12.64	.1400	.6103	1.96	.984	8.4
8.6	23.79	5.684	12.44	.1445	.5409	1.90	1.03	8.6
8.8	26.00	6.106	12.16	.1503	.4742	1.84	1.08	8.8
9.0	28.35	6.619	11.74	.1585	.4076	1.77	1.14	9.0
9.2	30.85	7.322	11.02	.1721	.3342	1.68	1.23	9.2
9.363	32.99	9.30	9.30	.2300	.2300	1.45	1.45	9.363

L.L.P.

N.B.P.

C.P.

NBS-
TN-
622
↓

NT=19, NP=16, M=304 POINTS

ENTHALPY

T = °R, P = PSIA

→ DIRECTLY FROM NBS-TN-622

T \ P	0.	0.1	0.5	0.730	1.0	4.	10.	20.
	30.	32.99	40.	45.	50.	100.	200.	300.
4.	11.35	11.34	11.16	11.05	1.443	1.499	1.610	1.794
	1.979	2.034	2.162	2.254	2.346	3.254	5.025	6.738
5.	12.60	12.59	12.45	12.36	12.28	2.038	2.135	2.301
	2.468	2.518	2.636	2.720	2.805	3.655	5.350	7.014
6.	13.84	13.84	13.72	13.65	13.58	12.95	2.723	2.867
	3.018	3.063	3.171	3.249	3.327	4.130	5.762	7.382
7.	15.08	15.08	14.98	14.92	14.85	14.36	13.08	3.612
	3.729	3.767	3.857	3.924	3.992	4.722	6.275	7.844
8.	16.32	16.32	16.22	16.17	16.11	15.71	14.77	4.689
	4.704	4.720	4.768	4.810	4.856	5.461	6.906	8.416
9.	17.56	17.56	17.47	17.42	17.37	17.03	16.26	14.61
	6.479	6.326	6.156	6.105	6.083	6.402	7.684	9.122
9.363	18.01	18.01	17.92	17.88	17.83	17.50	16.78	15.26
	12.21	9.30	7.60	7.00	6.80	6.819	8.006	9.411
10.	18.80	18.80	18.71	18.67	18.63	18.32	17.68	16.41
	14.70	14.00	11.31	8.929	8.203	7.550	8.572	9.917
11.	20.05	20.05	19.95	19.92	19.88	19.61	19.05	18.00
	16.76	16.33	15.17	14.16	12.99	8.936	9.529	10.75
12.	21.29	21.29	21.20	21.17	21.13	20.89	20.39	19.49
	18.49	18.16	17.33	16.68	15.97	10.76	10.60	11.66
13.	22.53	22.53	22.44	22.41	22.38	22.16	21.71	20.92
	20.07	19.80	19.13	18.63	18.10	13.14	11.81	12.66
14.	23.77	23.77	23.67	23.65	23.62	23.42	23.02	22.31
	21.57	21.33	20.77	20.36	19.93	15.68	13.17	13.75
15.	25.01	25.01	24.92	24.90	24.87	24.69	24.31	23.67
	23.01	22.81	22.32	21.96	21.59	17.91	14.71	14.93
16.	26.25	26.25	26.16	26.14	26.11	25.95	25.60	25.02
	24.42	24.24	23.80	23.49	23.17	19.94	16.40	16.21
18.	28.73	28.73	28.64	28.62	28.60	28.46	28.16	27.67
	27.17	27.02	26.66	26.40	26.14	23.56	20.08	19.07
20.	31.21	31.21	31.12	31.11	31.09	30.97	30.71	30.28
	29.84	29.71	29.41	29.19	28.97	26.79	23.73	22.31
24.	36.18	36.18	36.09	36.08	36.07	35.97	35.77	35.43
	35.10	34.99	34.76	34.59	34.42	32.76	30.17	28.82
30.	43.62	43.62	43.55	43.54	43.52	43.45	43.31	43.07
	42.84	42.76	42.60	42.48	42.36	41.20	39.22	37.95
36.	51.07	51.07	51.01	51.00	50.98	50.93	50.82	50.65
	50.48	50.43	50.31	50.23	50.14	49.31	47.85	46.80

CALCULATED	10.15.75	RHN	SPECIFIC ENTHALPY OF HELIUM (BTU/LB) AT LOW TEMPERATURE ≤ 20 K AIRESEARCH MANUFACTURING CO. LOS ANGELES, CALIFORNIA	FOR JTX PROGRAM
RECORDED				
DRAWN				
CHECKED				
APPROVED				

T = OR
P = PSIA

SPECIFIC VOLUME

**SPECIFIC VOLUME (FT³/LB)
OF HELIUM
AT LOW TEMPERATURE ≤ 20K**

**AIRESEARCH MANUFACTURING CO.
LOS ANGELES, CALIFORNIA**

VISCOSITY

$$P = P_{SIA}, \quad T = 0R$$

NP=10, NT=16, M=160 POINTS

[illegible]

THERMAL CONDUCTIVITY

$$NP = 8, NT = 20.$$

NP= 8, NT= 20, M=160 POINTS

M=160 POINTS

[illegible]

			THERMAL CONDUCTIVITY OF HELIUM (BTU/HR-FT-°R) AT LOW TEMPERATURE ≤ 20K	FOR JTX PROGRAM
CALCULATED	10.16-75	RHN		
RECORDED				
DRAWN				
CHECKED				
APPROVED			AIRESEARCH MANUFACTURING CO. LOS ANGELES, CALIFORNIA	

METAL THERMAL CONDUCTIVITY

NBS MONOGRAPH 131 (1973)

300-SERIES
STAINLESS STEEL

T (°R)	k (BTU/HR-FT-°R)
0	0
7.6	0.136
10.8	0.208
14.4	0.304
18.0	0.413
27	0.740
36	1.128
45	1.53
54	1.90
90	3.32

OFHC COPPER

T (°R)	k (BTU/HR-FT-°R)
0	0
3.0	20.
7.2	98.
10.8	173
14.4	243
18	312
27	462
36	578
45	642
54	653
63	624
72	578
90	491

CALCULATED	10.14.75	RHN
RECORDED		
DRAWN		
CHECKED		
APPROVED		

THERMAL CONDUCTIVITY OF
STAINLESS STEEL
AND OFHC COPPER (BTU/HR-FT-°R)
BELOW 50°K

AIRESEARCH MANUFACTURING CO.
LOS ANGELES, CALIFORNIA

FOR JTX
PROGRAM
S/R KEIN